Development 130, 3187-3204

doi:10.1242/dev.00548

The T-box-encoding Dorsocross genes function in amnioserosa development and the patterning of the dorsolateral germ band downstream of Dpp

Ingolf Reim, Hsiu-Hsiang Lee and Manfred Frasch*

Brookdale Department of Molecular, Cell and Developmental Biology, Mount Sinai School of Medicine, New York NY 10029, USA
*Author for correspondence (e-mail: manfred.frasch@mssm.edu)

Accepted 17 April 2003

SUMMARY

Dpp signals are responsible for establishing a variety of cell identities in dorsal and lateral areas of the early *Drosophila* embryo, including the extra-embryonic amnioserosa as well as different ectodermal and mesodermal cell types. Although we have a reasonably clear picture of how Dpp signaling activity is modulated spatially and temporally during these processes, a better understanding of how these signals are executed requires the identification and characterization of a collection of downstream genes that uniquely respond to these signals. In the present study, we describe three novel genes, *Dorsocross1*, *Dorsocross2* and *Dorsocross3*, which are expressed downstream of Dpp in the presumptive and definitive amnioserosa, dorsal ectoderm and dorsal mesoderm. We show that these genes are good candidates for being direct targets of the Dpp signaling cascade. Dorsocross expression in the dorsal ectoderm and mesoderm is metameric and requires a combination of Dpp and Wingless signals. In addition, a transverse stripe of expression in dorsoanterior areas of early embryos is independent of Dpp. The Dorsocross genes encode closely related proteins of the T-box domain family of transcription factors. All three genes are arranged in a gene cluster, are expressed in identical patterns in embryos, and appear to be genetically redundant. By generating mutants with a loss of all three Dorsocross genes, we demonstrate that Dorsocross gene activity is crucial for the completion of differentiation, cell proliferation arrest, and survival of amnioserosa cells. In addition, we show that the Dorsocross genes are required for normal patterning of the dorsolateral ectoderm and, in particular, the repression of *wingless* and the *ladybird* homeobox genes within this area of the germ band. These findings extend our knowledge of the regulatory pathways during amnioserosa development and the patterning of the dorsolateral embryonic germ band in response to Dpp signals.

Key words: T-box, Amnioserosa, Dorsal ectoderm, Dpp, *wingless*, *Drosophila*

INTRODUCTION

The BMP family member Dpp has a key role in dorsoventral axis formation and is responsible for the establishment of positional identities in dorsal and lateral areas of the early *Drosophila* embryo. Cell identities that are determined by Dpp include those of the extra-embryonic amnioserosa in the dorsalmost region of the embryo, dorsal epidermis and peripheral nervous system (PNS) in dorsolateral regions of the ectoderm, as well as dorsal vessel, dorsal somatic and visceral muscles in the dorsal mesoderm (Irish and Gelbart, 1987; Ray et al., 1991; Ferguson and Anderson, 1992a; Staehling-Hampton et al., 1994; Frasch, 1995). In addition to promoting dorsal epidermal and PNS fates in the dorsolateral ectoderm, Dpp acts to suppress the formation of neurons of the central nervous system in the same area.

For a better understanding of these activities, we need to consider that Dpp exercises some of its functions sequentially at different stages of development, during which *dpp* changes its own pattern of expression (St Johnston and Gelbart, 1987). In particular, during blastoderm and gastrulation stages, Dpp acts in a dose-dependent fashion to establish positional information in dorsal and lateral areas of the embryo and to specify amnioserosa tissue (Ferguson and Anderson, 1992a; Ashe et al., 2000). Although *dpp* is expressed uniformly around ~40% of the dorsal circumference of the embryos during this stage, the activity of Dpp is modulated along the dorsoventral axis by diffusion of the secreted gene product as well as by positive and negative regulators of the signaling pathway. Negative regulators include Short gastrulation (Sog) and Brinker (Brk), both of which are expressed ventrolaterally (Ferguson and Anderson, 1992b; Francois et al., 1994; Jazwinska et al., 1999). Whereas Sog and its vertebrate homolog Chordin are secreted molecules that inhibit BMP signaling via binding to the ligand (reviewed by Garcia Abreu et al., 2002), Brk appears to be a nuclear factor that interferes with the signaling output via binding to regulatory sequences of Dpp target genes (Sivasankaran et al., 2000; Kirkpatrick et al., 2001; Rushlow et al., 2001; Zhang et al., 2001). By contrast, specification of amnioserosa fates in the dorsal 10% of embryonic cells requires maximal signaling activities that involve Sog as a positive regulator of Dpp in conjunction with Twisted gastrulation (Tsg) as well as a second, uniformly-distributed BMP ligand, Screw (Scw) (Arora et al., 1994;

Mason et al., 1994; Ashe and Levine, 1999; Decotto and Ferguson, 2001). Dpp, Sog and Tsg are thought to be present in a diffusible trimolecular complex that serves to carry and release active Dpp prefentially into dorsalmost areas where *tsg* is expressed (Decotto and Ferguson, 2001).

After gastrulation, *dpp* expression ceases in the developing amnioserosa and becomes restricted to a broad stripe of cells in the dorsolateral ectoderm along the elongated germ band (St Johnston and Gelbart, 1987). During this period, the dorsally migrating cells of the mesoderm reach the *dpp*-expressing area of the ectoderm, thus allowing Dpp to induce dorsal mesodermal cell fates across germ layers (Staehling-Hampton et al., 1994; Frasch, 1995). In addition, Dpp is thought to act in the continuing patterning processes within the dorsolateral ectoderm during this stage, which lead to the specification of tracheal as well as particular epidermal and sensory organ progenitors. Both in the dorsal mesoderm and dorsolateral ectoderm, Dpp must act in combination with additional patterning molecules that provoke differential responses of cells to the Dpp signal. For example, in the dorsal mesoderm, the presence or absence of Wingless (Wg) activity determines whether cells will respond to Dpp by forming heart and dorsal somatic muscle progenitors versus visceral muscle progenitors (Wu et al., 1995; Azpiazu et al., 1996; Carmena et al., 1998).

In order to obtain more insight into the mechanisms of how Dpp signals pattern the embryo and how they are integrated with other patterning processes, it is crucial to study the regulation of Dpp target genes. To date, detailed molecular studies have been described for three targets that are induced during early embryogenesis, namely the homeobox genes *zerknüllt* (*zen*), *tinman* (*tin*) and *even-skipped* (*eve*). *zen* is required for the specification of the amnioserosa downstream of Dpp. Accordingly, the expression of *zen* in a dorsal on/ventral off pattern, although initially Dpp-independent, requires low levels of Dpp activity for its maintenance and high Dpp activities for its subsequent refinement to areas of the prospective amnioserosa (Doyle et al., 1986; Rushlow and Levine, 1990). Likewise, *tin* is required for the specification of all dorsal mesodermal tissues and *eve* for the normal differentiation of specific pericardial cells and dorsal somatic muscles in a Dpp-dependent manner. (Bodmer, 1993; Azpiazu and Frasch, 1993; Su et al., 1999). All three genes have in common the presence of multiple binding sites for intracellular Dpp effectors, the Smad proteins Mad and Medea, in their regulatory regions, which are essential for mediating the inductive activity of Dpp. However, in addition to these Smad-binding sites, each of these genes has a characteristic set of additional regulatory sequences that, at least in part, explain its particular spatial and tissue-specific response to Dpp signals. For example, *zen* contains binding sites for Brk in addition to the Smad sites (Rushlow et al., 2001). It appears that the antagonistic activities of the Brk and Smad sites and the differential ratios of Brk versus active Smad proteins along the dorsoventral embryo axis determine the ventral border of Dpp-dependent *zen* domain during cellularization stages. The Smad sites but not the Brk sites are also required for *zen* induction in the prospective amnioserosa during the cellularized blastoderm stage (Rushlow et al., 2001). The mesodermal Dpp targets *tin* and *eve* require Smad-binding sites and, in addition, binding sites for Tin, which serve to target the Dpp response to the mesoderm (Xu et al., 1998; Halfon et al., 2000; Knirr and Frasch, 2001). Further, the Dpp-responsive enhancer of *eve* contains functionally important binding sites for regulators that restrict its activity to segmental subsets of dorsal mesodermal cells, including the Wg effector Pangolin (Pan) (Halfon et al., 2000; Knirr and Frasch, 2001).

In the present study, we introduce three novel genes that respond to Dpp signals in the prospective amnioserosa, dorsal ectoderm and dorsal mesoderm, and are good candidates for being direct targets of the Dpp signaling cascade. The three genes, *Dorsocross1* (*Doc1*), *Dorsocross2* (*Doc2*) and *Dorsocross3* (*Doc3*), which are present in a gene cluster, are closely related members of the T-box family of genes and presumably arose by relatively recent duplications from a common ancestor. The Dorsocross (Doc) genes are expressed in essentially identical patterns within several areas that receive high levels of Dpp signals, including the prospective amnioserosa during the cellularized blastoderm stage, the dorsolateral ectoderm and dorsal mesoderm during germ band elongated stages and areas that span the compartment border in wing discs. We show that Doc expression in the prospective amnioserosa depends on *dpp* and *zen*, whereas the metameric expression in the dorsolateral ectoderm and dorsal mesoderm depends on a combination of *dpp* and *wg*. Our genetic analysis demonstrates that the three Doc genes have largely redundant functions during amnioserosa development, as well as during dorsolateral ectoderm and dorsal mesoderm patterning. We focus on the role of the Doc genes in the amnioserosa and dorsolateral ectoderm. We show that they are essential for full differentiation and maintenance of the amnioserosa, including the arrest of cell proliferation in this tissue. Owing to the requirement of a functional amnioserosa for normal germ band retraction, loss of Doc activity produces embryos with a permanently extended germ band. Hence, Doc genes are new members of the u-shaped family of genes. All genes of this family, which also includes *hindsight* (*hnt*; *peb* – FlyBase), *serpent* (*srp*), *tail-up* (*tup*), *u-shaped* (*ush*), *epidermal growth factor receptor* (*Egfr*) and *insulin-like receptor* (*InR*), are components of a regulatory network that controls normal development and functioning of the amnioserosa (Frank and Rushlow, 1996; Goldman-Levi et al., 1996; Yip et al., 1997; Lamka and Lipshitz, 1999). In addition to the amnioserosa, the Doc genes are required for the normal patterning of the dorsolateral ectoderm, which includes the repression of *wg* and *ladybird* (*lb*) expression within this area. These findings provide valuable insight into the mechanisms of how Dpp signals are executed during the development of the amnioserosa and the patterning of dorsolateral areas of the embryonic germ band.

MATERIALS AND METHODS

cDNA cloning and northern blots

660-850 bp DNA fragments from the non-conserved 3′-region of the predicted genes *CG5133* (*Doc1*), *CG5187* (*Doc2*) and *CG5093* (*Doc3*) were amplified by PCR from genomic DNA and cloned into pCRII-TOPO (Invitrogen) to obtain gene-specific probes. The following primer pairs were used: GTTCGCTAAGGGTTTCCGCG-AGTC and GCAAATAGTTTTGCATTTTCTACGGATTC for *Doc1*; GCGCTGCAAACGCAAGATGTCTTCATC and GCCGATATGCT-GAAGCCCTTGCTCCTT for *Doc2*; and GTCGAGATGCAAAC-GGAAGATCAATGAC and GTTTCATCCCAGAAATAGCTCCAT-

CGAATTCA for *Doc3*. A plasmid library containing cDNAs from 4- to 8-hour-old *Drosophila melanogaster* embryos in pNB40 (Brown and Kafatos, 1988) was screened with the respective radioactively labeled fragments and the plasmid DNAs of isolated clones were sequenced (GeneWiz, New York). The cDNAs shown in Fig. 1A correspond, from top to bottom, to clones Doc1-a1.1, Doc2-c6.2, Doc2-c1.1, Doc2-c12.2 and Doc3-b4.1.

Generation of Dorsocross antibodies

C-terminal cDNA fragments containing the variable coding region of each Dorsocross gene were cloned into the expression vector pQE-9 (Qiagen) cut with *Bam*HI and *Hin*dIII. Fragments were obtained by PCR using the cDNA clones Doc1-a1.1, Doc2-c6.2 and Doc3-b4.1 as templates and restriction site-introducing primers. In the recombinant proteins $Doc1^{CTD}$, $Doc2^{CTD}$ and $Doc3^{CTD}$, a N-terminal His-tag ($MGRSH_6GS$) is fused to an arginine residue at position 249, 246 and 249, respectively. Proteins were produced in *E. coli* M15{pRep4}. Expression was induced by 1 mM IPTG at mid-log phase and bacteria were grown for another 3-4 hours at 37°C, except for $Doc1^{CTD}$ that was produced at 30°C. Ni-NTA-agarose (Qiagen) purified proteins were used for immunization (Covance Research Products). Anti-Doc2 (made in rabbit) is specific for Doc2 in *Drosophila* embryos as shown by Doc1, Doc2 and Doc3 misexpression. Anti-Doc1 antibody (made in rat) reacts with Doc1 in *Drosophila* embryos, but only weakly at wild-type Doc1 levels. Unexpectedly, the two guinea pig antibodies derived from separate Doc2 and Doc3 immunizations both recognize both Doc2 and Doc3. Therefore, we name these antibodies anti-Doc2+3 and anti-Doc3+2, with anti-Doc2+3 working better for Doc3 detection.

Generation of *UAS*-Dorsocross transgenes

Transformation plasmids were constructed by subcloning the cDNAs Doc1-a1.1, Doc2-c6.2 and Doc3-b4.1 into pP{UAST} (Brand and Perrimon, 1993) using *Eco*RI or blunted *Eco*RI and *Not*I cloning sites. Doc1-a1.1 was cloned as *Eco*RI-*Not*I fragment, Doc2-c6.2 as *Sma*I-*Not*I fragment and Doc3-b4.1 as *Hin*dIII (blunted)-*Not*I fragment. The *Hin*dIII and *Not*I sites are pNB40 vector-derived and the *Eco*RI and *Sma*I sites are located in the 5′ UTR of *Doc1* and *Doc2*, respectively. Several independent lines were established for each construct using standard transformation methods (Rubin and Spradling, 1982). GAL4 inducible expression of Dorsocross proteins was confirmed by immunostaining with the antibodies described above.

Mutagenesis by male recombination

In order to create deletions uncovering all three Dorsocross genes a mutagenesis screen was performed using the male recombination method (Preston et al., 1996). The closest available *P*-insertion, *EP(3)3556*, was used to trigger male recombination in the presence of active transposase. *EP(3)3556* is a homozygous viable insertion in the 5′ region of *smg* (Dahanukar et al., 1999), which is located about 8 kb upstream of *Doc3* (see Fig. 6A). F0 males subject to recombination/mutagenesis carried both a X-chromosomal transposase source and the targeted *P*-insertion flanked by genetic markers on the third chromosome (*y w* H{PΔ2-3} HoP8/Y; *ru EP(3)3556 th st cu sr* e^s *ca*/+). F0 males were crossed to *ru h th st cu sr* e^s *Pr ca*/*TM6B, Bri Tb* females. The F1 generation was screened for non-balancer males carrying a recombinant third chromosome. The *ru* marker is expected to be retained along with the *P*-insertion if recombination causes a deletion extending towards the Dorsocross gene cluster (Preston et al., 1996). Recombinants were crossed individually to *Df(3L)Scf-R11*/ *TM3, Sb eve-lacZ* females for producing *TM3, eve-lacZ* balanced stocks and for complementation analysis with *Df(3L)Scf-R11*.

A total of 23 recombinants (13 *ru*, 6 *th st cu sr* e^s *ca* and four unusual marker combinations) were obtained out of 12400 scored non-balancer F1 males. These recombinants were derived from 18 of 168 individual F0 crosses and from each of these crosses only one *ru* male was taken to ensure the recovery of individual events. Five out of 10 candidate *ru* lines were homozygous lethal and two of them, *Df(3L)DocA* and *Df(3L)DocB*, removed the entire Dorsocross gene cluster. An analogous mutagenesis screen with *EP(3)584*, which is inserted ~80 kb downstream of *Doc1*, yielded *Df(3L)EP584MR2* (Fig. 5A).

Molecular characterization of deficiencies

The breakpoints of *Df(3L)DocA*, *Df(3L)DocB* and *Df(3L)EP584MR2* were mapped by sequencing of inverse PCR products recovered from the 5′ end of the retained *P* insertion. Inverse PCR was performed as described by E. J. Rehm (http:/www.fruitfly.org/p_disrupt/inverse_pcr.html) and Huang et al. (Huang et al., 2000) using Pwht1 and Plac1 primers. The removal of genes by various deficiencies (Fig. 5A) was confirmed by PCR from homozygous mutant embryos as described in Duan et al. (Duan et al., 2001). PCR from equally treated heterozygous embryos and PCR amplification of sequences not affected by the deficiencies served as positive controls for primers and template, respectively. PCR amplification and sequencing of DNA to the left of *EP(3)3556* demonstrated no change in sequences flanking the 3′ *P*-end.

TUNEL staining and BrdU labeling of embryos

Apoptotic cells were labeled by terminal deoxynucleotidyl transferase (TdT)-mediated dUTP nick end-labeling (TUNEL) using components of the ApopTag® Peroxidase kit S7101 (Intergen Company/Serologicals Corporation). Rehydrated embryos (about 30 μl) were treated with 10 μg/ml Proteinase K for 1 minute, rinsed quickly three times and washed another five times for 3 minutes with PBT. Embryos were postfixed in 3.7% formaldehyde in PBT for 20 minutes, washed five times with PBT and twice for 20 minutes with 30 μl equlibration buffer. TdT reaction was performed over night at 37°C using 50 μl buffer/TdT mixed in a ratio 7:3 and supplemented with 0.3% Triton X-100. The reaction was stopped by a 20 minute wash in 1/34 diluted stop buffer. Detection of incorporated Digoxigenin-nucleotides using sheep-anti-Dig and biotinylated anti-sheep antibodies, the VectaStain ABC elite kit (Vector Laboratories) and Tyramide Signal Amplification (TSA) reagents (NEN/Perkin Elmer Life Sciences) was essentially as for in situ hybridization using digoxigenin-labeled probes (Knirr et al., 1999).

BrdU labeling and detection was as described by Shermoen (Shermoen, 2000). Embryos were labeled by 30 minutes incubation in 1 mg/ml BrdU in PBS. For detection mouse anti-BrdU antibody (Becton-Dickinson, 1:200) and Cy3-anti-mouse antibody (Jackson ImmunoResearch Laboratories, 1:200) were used. For double staining, standard antibody staining using the VectaStain ABC elite kit and TSA fluorescence substrates were performed prior to the TUNEL reaction or BrdU detection.

Drosophila strains and crosses

y w or Oregon R were used as wild-type controls and stocks were obtained from the Bloomington stock collection unless noted otherwise. The following UAS/GAL4 driver lines were used: *P{GAL4-nanos.NGT} 40* (Tracey et al., 2000), *P{en2.4-GAL4} e22c*, *P{ZKr-GAL4}#8* (Frasch, 1995), *P{dpp.blk1-GAL4} 40C.6*, *P{w+mW.hs=GawB}c381* (Manseau et al., 1997) (which drives amnioserosa expression from stage 9; I.R. and M.F., unpublished) and *UAS-dpp#5* (Frasch, 1995). The following previously described mutant alleles were also used: dpp^{H46}, hnt^{E8}, pnr^{1}, *CyO* $slp^{\Delta 34B}$, $srp^{P\{PZ\}01549}$, tup^{1}, ush^{2}, wg^{CX4} and zen^{7}. For male recombination and mapping experiments, we used the lines *y w H{PΔ2-3} HoP8*, '*ru cu ca*' *and* '*ru Pr ca*', *ru Df(3L)Scf-R11, Scf-R6 th st cu sr e ca* (Kopp and Duncan, 1997), smg^{1} (Dahanukar et al., 1999), *Df(3L)29A6* kni^{ri-1} p^{p}, *EP(3)3556*, and *EP(3)584* (Exelixis). For ectopic expression experiments, embryos were collected at 28°C from crosses of *GAL4*-carrying females with UAS construct-carrying males. All other crosses were performed at room temperature (22-25°C).

RNA interference experiments

Sense and antisense RNA was transcribed from non-conserved 3′ fragments of *Doc1*, *Doc2* and *Doc3* in pCRII-TOPO (see above) and hybridized in injection buffer (5 mM KCl, 10 mM sodium phosphate, pH 7.8) to generate dsRNA (Kennerdell and Carthew, 1998). A mix of *Doc1*, *Doc2* and *Doc3* dsRNA (~100-300 pl of 4 mg/ml each) was injected ventrally into pre-blastoderm embryos that had been dechorionated and mounted onto double-sided sticky tape under Halocarbon 700 oil. An Eppendorf FemtoJet automatic injector and Eppendorf Femtotip injection needles were used for injections. Embryos were allowed to develop at 18°C until the desired stage was reached. For immunostaining, embryos were transferred to standard heptane/formaldehyde fixation solution in a small drop of oil. The heptane phase and total fixation solution were exchanged twice to remove traces of oil. After 20 minutes incubation, the formaldehyde solution was replaced by PBS. For the manual removal of the vitelline membranes, embryos were spread on agar plates, transferred to double-sided sticky tape and covered with PBS. After devitellinization 0.05% Tween was added and embryos were transferred into reaction tubes for standard staining procedures. Cuticle preparations were made 2-3 days after injection. Embryos were passed through acetic acid/glycerol (4:1) overlaid with heptane, transferred to a mesh, rinsed with heptane and PBT and mounted in standard Hoyer's medium.

Staining of embryos and imaginal discs

Antibody staining of embryos using DAB, double fluorescent staining and in situ hybridization in combination with fluorescent antibody staining were carried out as described previously (Knirr et al., 1999). Dorsocross in situ hybridization probes were made by in vitro transcription from 3′ fragments cloned into pCRII-TOPO (see above). The *race* in situ hybridization probe and *zen* cDNA were a gift from C. Rushlow (Frank and Rushlow, 1996). Antibody staining of imaginal discs was essentially the same as for embryos, except that imaginal discs attached to inverted larval heads were fixed in 3.7% formaldehyde in PBS, dehydrated in methanol, and rehydrated using 70%, 50% and 30% methanol in PBT before blocking and staining.

The following antibodies were used: rabbit anti-Doc2 (1:2000), guinea pig anti-Doc2+3 (1:400 to 1:600), guinea pig anti-Doc3+2 (1:600), rat anti-Doc1 (1:200), rabbit anti-Bap (1: 500) (Zaffran et al., 2001), rabbit anti-β-galactosidase (Promega; 1:1500), rabbit anti-Phospho-Smad1/PMad (1:2000; gift from C.-H. Heldin), rat anti-Cf1a (1:3500; gift from W. A. Johnson, University of Iowa), guinea pig anti-Kr (1:400) (Kosman et al., 1998), guinea pig anti-Slp (1:20) (Kosman et al., 1998), affinity-purified rabbit anti-C15 (1:25 to 1:50, TSA-indirect, NEN; S. Grimm and M.F., unpublished), mouse monoclonal anti-Lbe (1:10) (Jagla et al., 1997), and rabbit anti-phospho-Histone H3 (1:600; Upstate Biotechnology, NY). Monoclonal mouse antibodies obtained from the Developmental Studies Hybridoma Bank, University of Iowa: anti-α-tubulin 12G10 (1:10), anti-Futsch 22C10 (1:250), anti-Wg 4D4 (1:40, in imaginal discs 1:400), anti-En/Inv 4D9 (1:4), anti-Hnt 27B8 1G9 (1:30) and anti-β-gal 40-1a (1:40).

RESULTS

Three novel T-box genes are clustered in the chromosomal region 66F1-2

Sequence information from the Berkeley *Drosophila* Genome Project (Adams et al., 2000) revealed that three novel, closely related T-box encoding genes are clustered within ~40 kb of genomic sequences at 66F1 to 66F2 on chromosome arm 3L. In reference to their peculiar patterns of expression in blastoderm embryos (see below), these genes have been named, from proximal to distal, *Dorsocross1* (*Doc1*; previously *Tb66F2*) (Lo and Frasch, 2001), *Dorsocross2* (*Doc2*) and *Dorsocross3* (*Doc3*) (Fig. 1A). The gene cluster also includes an unrelated predicted gene, *CG5194*, which maps between *Doc2* and *Doc3*.

cDNAs for the three Doc genes, which were isolated from an early embryonic cDNA library (see Materials and Methods), encode proteins of 391 amino acids (Doc1), 469 amino acids (Doc2) and 424 amino acids (Doc3), respectively. Comparisons between cDNA and genomic sequences indicate that *Doc2* encodes at least three different mRNA products, which appear to be generated from alternative transcription start sites. Among these, *Doc2* variants A and B encode identical polypeptides, whereas variant C does not encode any long open reading frame (Fig. 1A). The data from northern analysis indicate that the longest cDNAs obtained for each gene are close to full length if the polyA tails are taken into account (1.7 kb transcripts versus 1500 bp cDNA for *Doc1*, 2.0 kb transcripts versus 1759 bp cDNA for *Doc2*A, and 1.8 kb transcripts versus 1681 bp cDNA for *Doc3*) (data not shown). For *Doc2*, these data indicate that variant A (1.75 kb, presumably corresponding to the 2.0 kb transcripts) is expressed much more strongly than the other two variants. In addition, we note that splicing occurs at identical positions within the open reading frames of *Doc1*, *Doc2* and *Doc3*, although most introns in *Doc3* are much smaller as compared with those in the other two genes (Fig. 1A).

Sequence comparisons show that the three Doc proteins share high degrees of similarity within their T-box domain sequences (>95% amino acid identities) as well as within short sequence stretches extending N- and C-terminally from these domains (Fig. 1B). The N-terminal regions of the polypeptides up to the T-box domains are moderately conserved (>40% amino acid identities), whereas the C-terminal regions contain only few short stretches of additional sequence similarity (data

Fig. 1. Genomic clustering, gene structure and phylogenetic analysis of the T-box genes *Doc1*, *Doc2* and *Doc3*. (A) Arrangement of the three Dorsocross genes within a genomic region of about 40 kb. *CG5194* is a predicted gene with no similarity to any known gene. The exon structures of Doc cDNAs are depicted below with the coding sequences hatched and the T-box domains in black. The exon-intron structure with the T-box spanning exons 2 to exons 5 is conserved among *Doc1*, *Doc2* variant A and *Doc3*. (B) ClustalX-generated alignment of T-box domains from T-box genes of *Drosophila melanogaster* (*Doc1*, *Doc2*, *Doc3*, *omb*/*optomotor-blind*, *H15*, *H15r*/*H15-related*/*CG6634*, *org-1*/*omb-related gene 1*, *byn*/*brachyenteron*/*trg*) and human (marked Hs). Additional Tbx6/16-related members of the T-box family, which appear to form a separate subgroup, are included from zebrafish (Dr) and *Xenopus laevis* (Xl). The T-box core sequence was N- and C-terminally extended in order to include amino acids partially conserved between subfamily members. (C) Phylogenetic N-J tree derived from ClustalX analysis, based on the alignment shown in B and using 1000 bootstrap trials (bootstrap values at tree node represent confidence values; branches with values below 700 are generally considered as less reliable and below 500 as unreliable. Bar represents amino acid exchanges as a fraction of 1). *Caenorhabditis elegans* (Ce) Tbx9 was included as an outgroup member. GenBank Accession Numbers are, for *Doc2A*, AAM11544; for *Doc2B*, AAM11545; and for *Doc3*, AAM11543. A Doc1 protein sequence identical to ours has previously been submitted by R. Murakami and T. Hamaguchi (AB035412).

A
Doc3
CG5194
Doc2
Doc1
1 kb
18 kb
T-Box
ATG
Stop
Doc1
Doc2
variant A
Doc2
variant B
Doc2
variant C
Doc3
B
C
Tbx6 subfamily
VegT subfamily
Tbx2 subfamily
Tbx1 subfamily
T subfamily
Tbr subfamily
Doc1
Doc3
Doc2
HsTbx6
DrTbx6
XlTbx16/VegT
DrTbx16/spadetail
Omb
HsTbx3
HsTbx2
HsTbx5
HsTbx4
H15r
H15
HsTbx20
Org-1
HsTbx1
HsTbx22
HsTbx18
Byn
HsBra/T
HsTbx21
HsTbr1
HsTbr2
CeTbx9
0.05

not shown). Additional sequence comparisons with T-box domains from vertebrates and phylogenetic analysis show that the Doc T-box domains are most closely related to those from members of the Tbx6 subfamily of T-box proteins (Fig. 1B,C) (Papaioannou, 2001) (see Discussion).

Dorsocross expression is prominent in dorsal tissues during embryogenesis

Northern analysis with gene-specific probes showed that all three Doc genes display similar expression profiles during development with maximal levels occurring between 2 and 12 hours of embryonic development and lower levels during late embryonic, larval and pupal stages. The only significant difference among the three genes in this assay was the expression of *Doc1* mRNA in adult males, which was not observed for *Doc2* and *Doc3* (data not shown).

The spatial expression patterns of Doc products in embryos were examined by whole-mount in situ hybridization with gene-specific probes and whole-mount immunocytochemistry using antibodies raised against the unique C-terminal regions of the Doc proteins (see Materials and Methods). As all three genes were found to have essentially identical expression patterns (with some minor differences regarding the relative levels of expression in different tissues; data not shown), we will henceforth collectively refer to them as 'Doc genes'. As expected, Doc proteins are exclusively nuclear during interphase.

The initial expression of Doc genes is observed at the cellular blastoderm stage in a transverse stripe encompassing the dorsal ~40% of the embryonic circumference within the prospective head region. Shortly later, a narrow longitudinal stripe of expression appears, which ultimately extends all along the dorsal midline of the embryo, and the joint domains form a cross-shaped pattern of Doc expression in dorsal areas of the early embryo (Fig. 2A). The domain of the transverse stripe is located anteriorly to the cephalic furrow forming during gastrulation (Fig. 2B; Fig. 3G) and largely corresponds to procephalic neuroectoderm. The cells of this domain continue Doc expression until stage 11, when the segregation of procephalic neuroblasts is completed (Fig. 2B-D) (Campos-Ortega and Hartenstein, 1997). By contrast, the cells from the dorsal longitudinal domain within the trunk region give rise to amnioserosa, which maintains strong Doc expression until stage 15 (Fig. 2C-F). In addition, the cells from the anterior and posterior termini within this longitudinal stripe contribute to regions of the anterior and posterior digestive tract and maintain expression until stage 11.

During stages 9 and 10, a new pattern of Doc expression emerges within dorsolateral areas of the germ band from parasegment (PS) 1 to PS13, which consists of 13 rectangular cell clusters (Fig. 2D). This metameric expression includes ectodermal as well as underlying mesodermal cells. In the ectoderm, Doc expression is excluded from the dorsalmost cells near the amnioserosa at this stage, whereas in the ectoderm the metameric Doc expression extends to the dorsalmost areas of this germ layer (Fig. 2D; see below). To determine the segmental register of Doc expression in the mesoderm we co-stained with antibodies against the POU domain transcription factor Cf1a (Vvl – FlyBase), which mark the tracheal placodes (Anderson et al., 1995). As shown in Fig. 2E, Doc and Cf1a are expressed in mutually exclusive domains, which implies that Doc expression encompasses prospective tissues of the lateral epidermis and dorsolateral sensory organs. After stage 11, the segmental expression in the epidermis is modified to form segmental stripes that are interrupted in dorsolateral regions. Within these stripes, Doc expression is largely found in posterior areas of the anterior compartments of each segment and there is a graded distribution of Doc expression with increasing levels towards the posterior of each stripe (Fig. 2F,G). The dorsal epidermal expression domains now extend to the amnioserosa, and after dorsal closure the bilateral domains merge at the dorsal midline (Fig. 2F-H).

Additional sites of Doc expression during late embryogenesis include the dorsal pouch in the embryonic head (Fig. 2H), the anterior pair of Malpighian tubules (Fig. 2I) and the pentascolopidial chordotonal sensory organs (Fig. 2J). The mesodermal expression of the Doc genes, which will be presented elsewhere in more detail along with functional data, is observed in areas between the expression domains of the homeobox gene *bagpipe* (*bap*) at stage 10 (Fig. 2K). This location defines them as dorsal areas of the mesodermal A (or slp) domains (Azpiazu et al., 1996; Riechmann et al., 1997), which include the dorsal somatic and cardiogenic mesoderm. During early stage 11, additional Doc expression initiates in the caudal visceral mesoderm, which contains the founder cells of the longitudinal muscles of the midgut (Fig. 2L) (San Martin et al., 2001; Klapper et al., 2002). As reported previously for *Doc1*, two out of six bilateral cardioblasts in each segment of the dorsal vessel, which are *tin* negative and *svp* positive, also express the Doc genes (Fig. 2H) (Lo and Frasch, 2001).

Doc expression along the dorsal midline depends on *dpp* and *zen*

As peak levels of Dpp activity are known to be required for cell fate determination at the dorsal midline, we tested whether there is a correlation between Dpp activity and dorsal longitudinal Doc expression during blastoderm stages. As shown in Fig. 3A, double-staining for Doc mRNA and phosphorylated Mad (PMad) indicates a close correlation between cells containing high levels of PMad and Doc products within the dorsal-longitudinal stripe. In addition, faint Doc signals that are modulated in a pair-rule pattern extend into areas that receive lower Dpp inputs and lack detectable PMad (Fig. 3A). As predicted, both PMad and Doc expression in the dorsal-longitudinal stripe, but not the dorsal-transverse head stripe of Doc expression, are absent in *dpp*-null mutant embryos (Fig. 3B). Conversely, in blastoderm embryos with ubiquitous Dpp expression (*UAS-dpp* activated by maternally provided *nanos-GAL4*), we observe a significant widening of the dorsal-longitudinal stripes of PMad and Doc expression, during which the correlation between high PMad and Doc mRNA levels is still maintained (Fig. 3C).

The expansion of PMad upon uniform ectopic expression of *dpp* includes the prospective mesoderm, although not ventrolateral areas of the blastoderm embryo (Fig. 3D). However, high PMad in the prospective mesoderm does not trigger ectopic Doc expression, suggesting either the presence of a ventral repressor or the requirement for a co-activator in dorsal areas. A candidate for a co-activator is the homeobox gene *zerknüllt* (*zen*). Double in situ hybridization shows that the appearance of dorsal Doc mRNAs coincides with the time

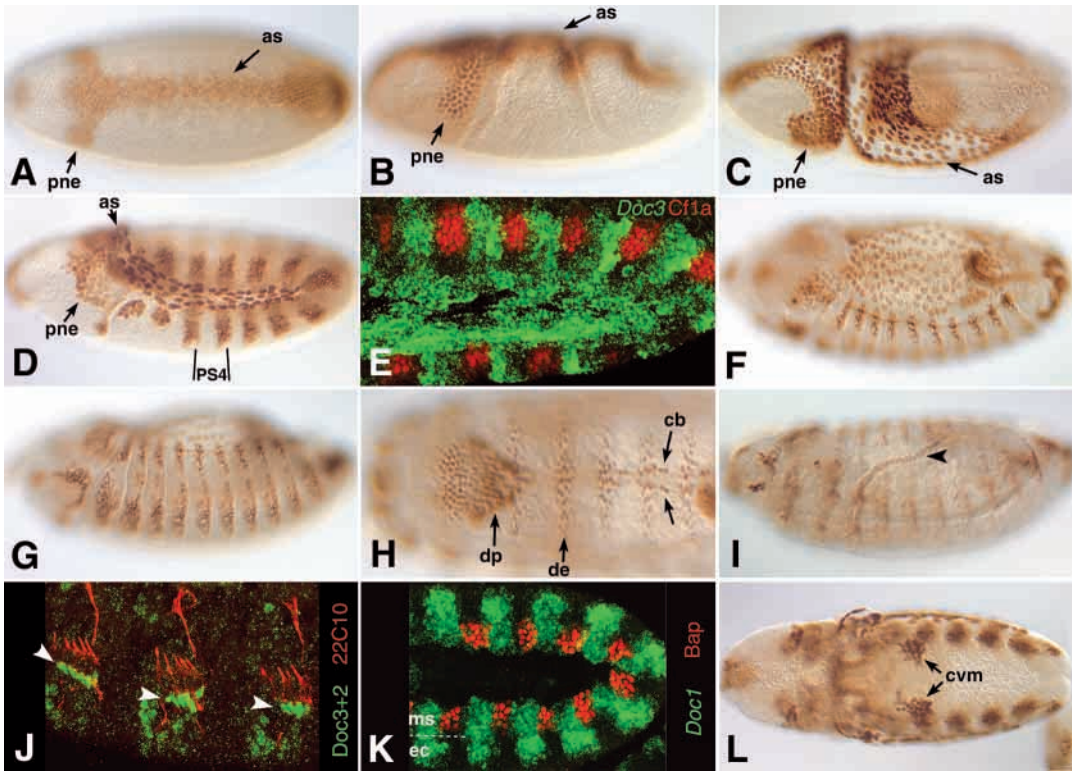

Fig. 2. Embryonic expression pattern of Dorsocross. Nuclear Dorsocross proteins were detected by immunostaining with anti-Doc3+2 antibody (see Materials and Methods) and visualized either with DAB (brown in A-D,F-I,L) or fluorescent secondary antibodies (J). Dorsocross mRNA was detected by in situ hybridization with specific probes for *Doc3* (E) or *Doc1* (K). Images from fluorescent staining are combined ectodermal (E), subepidermal (J) or mesodermal (K) confocal sections. Views are lateral (B,D,E,G,I-K) or dorsolateral (C,F) with dorsal upwards and anterior towards the left, or dorsal with anterior towards the left (A,H,L). Embryos are oriented the same way in all figures and all non-flourescent images are taken using Nomarski optics.
(A) Blastoderm stage embryo, (B) stage 7 embryo and (C) stage 8 embryo showing Dorsocross protein in the anlagen of the amnioserosa (as) and the procephalic neuroectoderm (pne). Amnioserosa nuclei are distinguishable by their larger size. (D) At stage 10, a metameric expression pattern (PS4, parasegment 4) has emerged in addition to continued expression in the amnioserosa. (E) Patches of Dorsocross expression (green) alternate with the tracheal placodes labeled by anti-Cf1a antibody staining (red) in the dorsolateral ectoderm of the embryonic trunk. (F,G) At stage 14, epidermal stripes are visible dorsally and ventrolaterally. (H) Enlarged view of stage15-16 embryo that has completed dorsal closure, showing expression in dorsally fused epidermal stripes (de) and in the dorsal pouch (dp), and two pairs of cardioblasts per segment (cb). (I) Stage 16 embryo focussed on Doc expression in Malpighian tubules (arrowhead). (J) Dorsocross expression in the pentascolopidial chordotonal organs (arrowheads, green), which are marked by their staining with mab 22C10 (red). Dorsocross-positive cells are identified as ligament cells based on their ventral juxtaposition to 22C10-labeled LCh5 neurons (arrowheads). Some epidermal Doc staining is also present in this image. (K) The metameric expression as seen in D includes the dorsal mesoderm, where Dorsocross-expressing cells (green) alternate with visceral mesoderm precursors that express *bap* (red). The combined sections include ectodermal expression seen in more radial areas [see broken line between mesoderm (ms) and ectoderm (ec)]. (L) Stage 11 embryo focussed on the bilateral caudal visceral mesoderm anlagen (cvm) close to the posterior tip of the germ band.

when *zen* mRNA levels increase in the areas of the presumptive amnioserosa as a result of high Dpp inputs (Fig. 3E). When the refinement of *zen* expression is completed, there is an exact correspondence in the widths of the Doc and *zen* expression domains, although Doc expression extends more posteriorly (Fig. 3F). As shown in Fig. 3H (compare with Fig. 3G), the activity of *zen* is necessary for normal levels of Doc expression in the dorsal-longitudinal stripe, because in *zen* mutant embryos there are only low residual levels of Doc products present in this domain. These observations suggest that Doc expression along the dorsal midline of blastoderm embryos requires the combined activities of *dpp* and *zen*.

Metameric Doc expression in dorsal ectoderm and mesoderm requires Dpp + Wg

The known distribution of *dpp* mRNA during its second phase of expression in the dorsolateral ectoderm of stage 9-11 embryos (St Johnston and Gelbart, 1987) suggests that Doc expression in the dorsolateral ectoderm and mesoderm during these stages is also dependent on Dpp activity. As expected from the known fate map shifts in *dpp* mutants, these domains of Doc expression are missing in *dpp*-null mutant embryos (data not shown). Notably, the exact coincidence between the ventral borders of the domains of dorsolateral Doc expression and high nuclear PMad (Fig. 4A,B) suggests that Doc expression is directly controlled by Dpp-activated Smad proteins in the ectoderm and mesoderm during this stage. Additional evidence for this hypothesis comes from experiments with ectopic expression of *dpp* in the ventral ectoderm of the Krüppel domain (by virtue of a modified *Kr-GAL4* driver) (Frasch, 1995), which results in the concomitant expansion of PMad and the Doc expression stripes towards the ventral midline (Fig. 4C).

In addition to the inputs from *dpp*, metameric Doc expression in dorsolateral areas of the germ band must depend on the activity of segmental regulators. A direct comparison with the expression of *engrailed* (*en*) shows that the clusters of Doc expression straddle the compartmental borders. Although Doc expression overlaps with *en* in the P compartments, about two-thirds of the Doc expressing cells of each cluster are

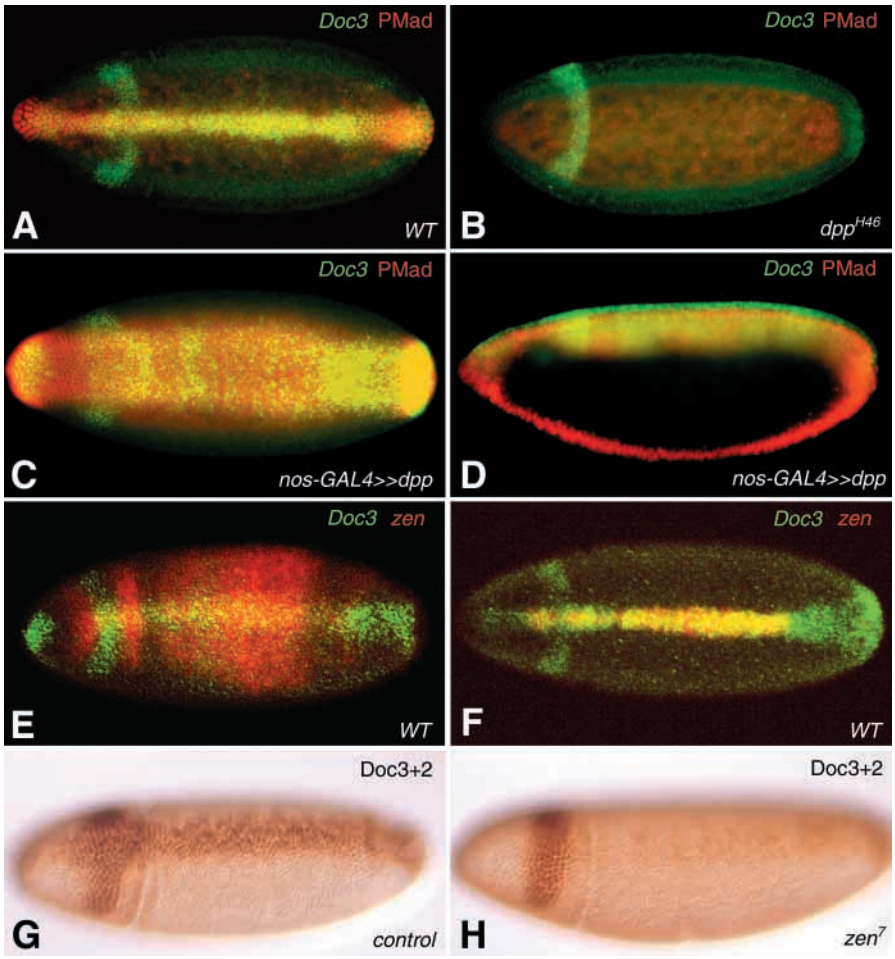

Fig. 3. Dorsocross expression along the dorsal midline of blastoderm stage embryos requires *dpp* and *zen*. (A-D) Double-fluorescent staining for *Doc3* RNA and nuclear Phospho-Mad (PMad) protein. An antibody specific for the activated (phosphorylated) form of the Dpp effector Mad allows monitoring Dpp activity. All views are dorsal, except the lateral view in D. The longitudinal stripe is absent from homozygous dpp^{H46} embryos (B) when compared with the wild type (A). (C,D) Upon induction of ectopic Dpp via *P{GAL4-nanos.NGT}40* and *UAS-dpp*, nuclear PMad and expression of *Doc3* (as well as of *Doc1* and *Doc2*, not shown) appear in a significantly broader longitudinal stripe when compared with A. PMad, but not *Doc3*, is also detected in ventral cells (D). (E) Double in situ hybridization for *Doc3* mRNA (green) and *zen* mRNA (red) shows that the dorsal stripe of Doc expression appears during the time when refined *zen* expression is detected on top of the weaker broad *zen* pattern. (F) During mid stage 5, when *zen* transcripts in the broad dorsal domain have disappeared, and dorsal *Doc3* and *zen* are expressed at peak levels, the widths of the *Doc3* and *zen* domains are identical. (G) Dorsolateral view of heterozygous zen^{7}/*CyO* embryo and (H) homozygous *zen*$^{-}$ mutant (zen^{7}, also known as zen^{W36}) stained with anti-Doc3+2 antibody. Very little Dorsocross protein is detectable along the dorsal AP axis in *zen* mutants. By contrast, expression is maintained in the head stripe and at the termini (foregut and hindgut primordia, more prominently at later stages). Embryos in A,B,G,H were analyzed at the beginning of gastrulation, when wild-type embryos have a fully formed dorsal stripe.

located in posterior areas of the A compartments (Fig. 4D). In agreement with this allocation, we find that the metameric Doc domains are exactly centered on the stripes of Wingless (Wg) expression (Fig. 4E). The observed correlation of the segmental registers of Wg and Doc makes *wg* a good candidate for an upstream regulator of Doc. As shown in Fig. 4F, dorsolateral Doc expression in the ectoderm and mesoderm is completely absent if *wg* is inactive. By contrast, deletion of *sloppy paired* (*slp*), a known target of *wg* in the mesoderm and a *wg* feedback regulator in the ectoderm (Lee and Frasch, 2000), results in a reduction, but not a complete loss of metameric DOC expression (data not shown). Hence, *slp* probably affects Doc indirectly through its effect on ectodermal *wg* expression. Altogether, our data suggest that metameric Doc expression in the ectoderm and mesoderm is triggered by the intersecting activities of Wg and Dpp.

The Doc genes are required for full differentiation and maintenance of amnioserosa cells

The similarities in sequence and expression of the three Doc genes suggested functional redundancy among these genes. Because our molecular analysis of available deficiencies at 66E-F showed that none of them uncovered all three genes (Fig. 5A) we used the flanking P-insertions *EP(3)3556* and *EP(3)584* in attempts to delete the entire Doc gene cluster via male recombination-induced mutagenesis (see Materials and Methods). Molecular mapping of the obtained deletions demonstrated that two of them, *Df(3L)DocA* and *Df(3L)DocB*, which were generated with the distally located insertion *EP(3)3556* and cause embryonic lethality, deleted all three Doc genes (Fig. 5A). As *Df(3L)DocA* deletes the smallest number of additional genes (*CG5087*, *CG5194*, *CG5144*, *Argk* and *CG4911*), we describe the phenotypic analysis in the present study using this deficiency, although the salient phenotypes are very similar between *Df(3L)DocA* and *Df(3L)DocB*.

Additional genetic analysis showed that it is possible to obtain a small number of viable adult escapers with the genotype *Df(3L)Scf-R11*/*Df(3L)DocA*, which indicates that *CG5087* is not absolutely required for viability, and that *Doc1* and *Doc2* can functionally substitute for the loss of *Doc3*. Similarly, the full viability of flies with the genotype *Df(3L)DocA*/*Df(3L)EP584MR2* (Fig. 5A) shows that *CG4911* and the 5′ exons of *Argk* (preceding the large intron) are also not essential. Furthermore, we determined that embryos with the genotypes *Df(3L)Scf-R11*/*Df(3L)DocA* and *Df(3L)DocA*/*Df(3L)29A6* (which causes pupal lethality) do not display any of the phenotypes described below for *Df(3L)DocA* homozygous embryos. In summary, our genetic analysis shows

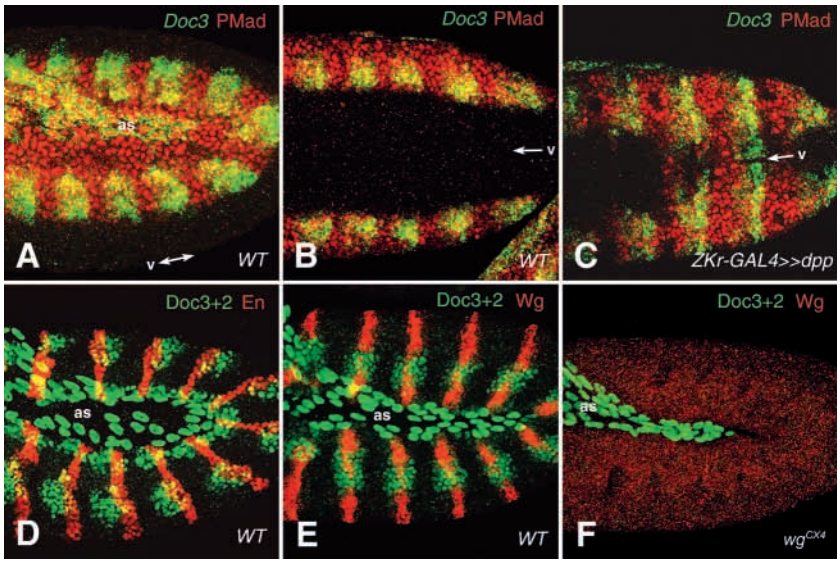

Fig. 4. Combinatorial inputs from Dpp and Wg signaling regulate metameric Dorsocross expression in the dorsolateral ectoderm and mesoderm. (A,B) *Doc3* in situ hybridization (green) and anti-PMad antibody staining (red) in wild-type stage 10 embryos seen from lateral (A) or ventral (B) views (only trunk regions are shown in this figure; v, ventral midline). *Doc3* expression is activated within the nuclear PMad domain. (C) Ventral extension of the ectodermal PMad domain by ectopic Dpp leads to ventral extension of *Doc3* patches. Ectopic Dpp was driven from a UAS-*dpp* transgene by *ZKr*-GAL4 in the ectodermal Krüppel domain (Frasch, 1995). (D,E) Wild-type stage 10-11 embryos double-stained with anti-Doc3+2 antibody (green) plus anti-En/Invected (red) (D) and anti-Doc3+2 antibody (green) plus anti-Wg (red) (E). Ectodermal Doc expression is centered around the Wg-stripes and overlaps partially with the En stripes (yellow ectodermal signals). (F) Homozygous wg^{CX4} mutant embryo stained as in E. Metameric Doc expression is absent from the ectoderm and mesoderm, although amnioserosa expression is not affected. All images are combined confocal sections within the specified germ layer. Doc-expressing cells flanking the amnioserosa (as) in D, and to lesser extent in E, are mesodermal.

that the loss of either *Doc3* or *Doc1* can be compensated for by the remaining two Doc genes in embryos and that the phenotypes described herein are a consequence of the loss of all three of the Doc genes. However, we can not rule out a contribution of *CG5194*, which encodes a 128 amino acid predicted ORF with no known homology, to the observed phenotypes.

Because of the prominent Doc expression in the primordia and developing tissue of the amnioserosa we used the amnioserosa marker *Krüppel* (*Kr*) to examine whether the Doc genes are required for the development of this extra-embryonic tissue. These experiments demonstrated that homozygous *Df(3L)DocA* mutant embryos (henceforth called *DocA* mutants) fail to express *Kr* in the amnioserosa at any stage, whereas CNS expression of *Kr* is not affected (Fig. 5B). To confirm that this observed phenotype is due to the loss of Doc gene function we diminished Doc gene functions by using RNA interference (RNAi) as an independent assay and performed rescue experiments with *DocA* mutants (see below). As shown in the example of Fig. 5C, injection of a mixture of equimolar amounts of dsRNAs for all three Doc genes (see Materials and Methods) frequently results in a complete absence of *Kr* expression in the amnioserosa. The remaining embryos display strongly reduced numbers of Kr-containing nuclei in this tissue (data not shown). These phenotypes correlate with the observed absence or severe reduction of Doc protein levels in Doc RNAi embryos (data not shown). By contrast, mock-injected embryos display normal expression of *Kr* in the amnioserosa (Fig. 5D). Hence, the strongest phenotype obtained by RNAi mimics the observed *DocA* mutant phenotype, confirming that the lack of *Kr* expression in *DocA* mutant embryos is specifically due to the loss of the activity of all three Doc genes.

Besides the effects on *Kr* expression, *DocA* mutant and RNAi-treated embryos share several morphological defects. The extending germ band is unable to displace the amnioserosa fully towards the anterior and the posterior germ band is therefore forced to bend underneath the amnioserosa. Of note, germ band retraction is strongly disrupted, which can be clearly seen in stage 14 embryos (Fig. 5E) and in cuticle preparations of unhatched first instar larvae (Fig. 5H,I; compare with J). This phenotype is shared with previously described genes of the u-shaped (ush) group, which affect the maintenance of the amnioserosa (Frank and Rushlow, 1996). Kr expression and the germ band retraction defects in *DocA* mutant embryos can be partially rescued by expressing any of the three Doc genes with an early amnioserosa-specific driver (Fig. 5F,G). Rescue with *Doc2* (Fig. 5F) is consistently more efficient when compared with *Doc1* (data not shown) and *Doc3* (Fig. 5G), although it is not known whether this difference is due to a higher intrinsic activity or a more efficient expression of Doc2 protein in this assay.

An additional phenotype consists of reductions in the size of the embryonic head in *DocA* mutants and RNAi-treated embryos, which is apparent from stage 12 onwards and results in reduced head structures and a frequent failure of head involution at later stages (Fig. 5B,C,H,I, and data not shown). This phenotype is probably due to excessive cell death as a consequence of the absence of Doc activity in the procephalic neuroectoderm and other dorsal areas of the embryonic head (Fig. 2B,C and data not shown). The observed head phenotypes, as well as the aberrant shape of the filzkörper (Fig. 5I), are also reminiscent of similar phenotypes of embryos mutant for genes of the ush group (Frank and Rushlow, 1996).

To obtain more information about the particular role of the Doc genes in the specification and/or differentiation of the amnioserosa we analyzed the distribution of additional amnioserosa markers in *DocA* mutant embryos. For the ush group gene *hnt* (Yip et al., 1997) we find a strong reduction of expression, with significant levels of Hnt protein only being detected in nuclei along the posterior margin of the amnioserosa (Fig. 6A, Fig. 7A, compare with Fig. 6B and Fig. 7B, respectively). By contrast, the expression of the

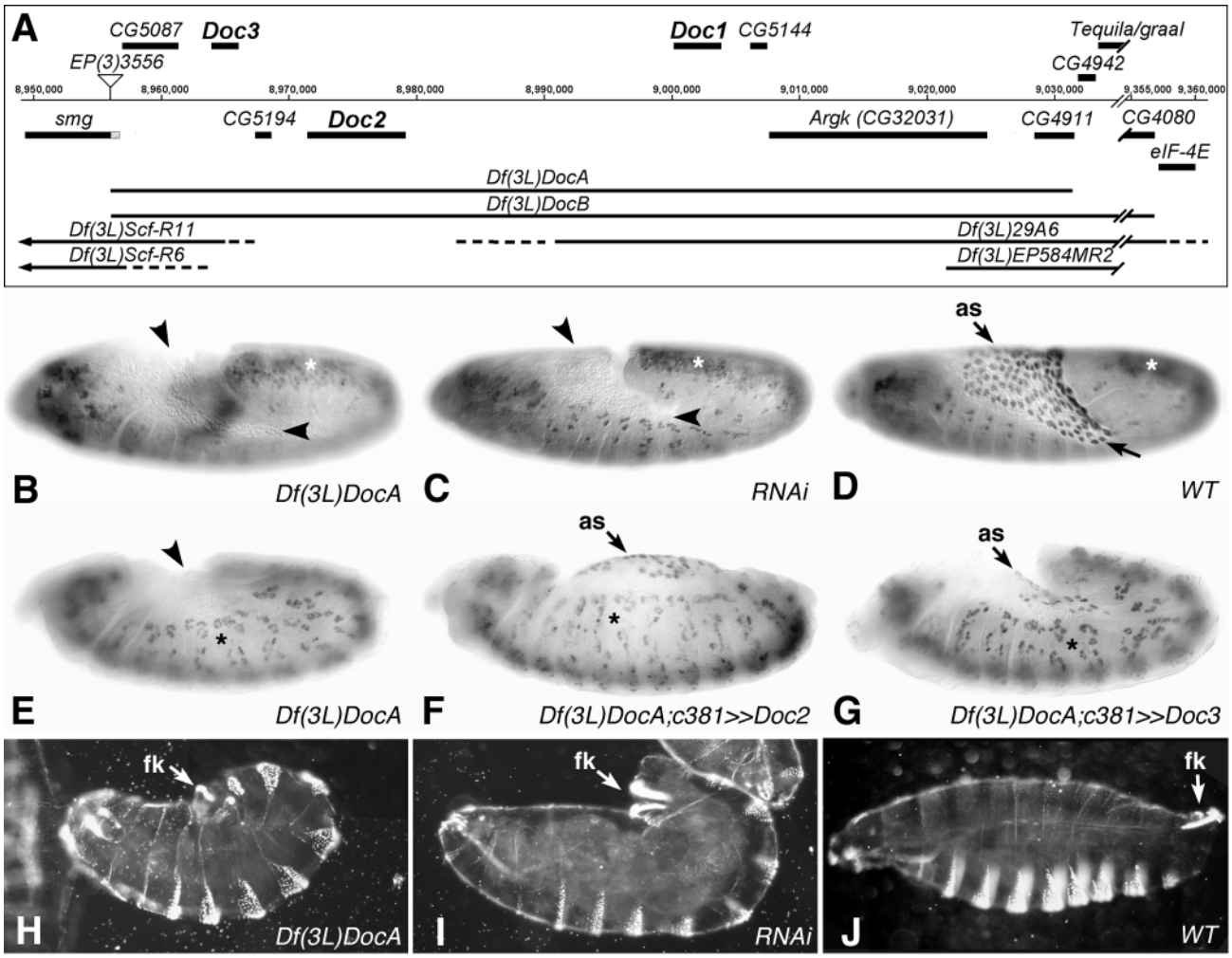

Fig. 5. Mutagenesis of the Dorsocross locus and phenotypic rescue experiments. (A) Genomic map of the Dorsocross region showing known and predicted genes, deficiencies and *P*-insertions. Numbers indicate base pair coordinates of genomic sequences on chromosome 3L (BGPD release 3). Slashes indicate the omission of sequences owing to space limitations. Genes above the genomic line are transcribed from left to right and those below from right to left (introns are not displayed). *EP(3)3556* was used for generating *Df(3L)DocA* and *Df(3L)DocB*, and EP(3)584 (male-sterile insertion in *bol*, located within the omitted sequence) for *Df(3L)EP584MR2*. Relevant breakpoints of previously known deficiencies were mapped by PCR from homozygous embryos. Dashes indicate uncertainty ranges of breakpoints. In situ hybridization confirmed the presence of mRNAs of all three Doc genes in *Df(3L)Scf-R6*, absence of *Doc3* mRNA in *Df(3L)Scf-R11*, absence of *Doc1* mRNA in *Df(3L)29A6*, and absence of all three Doc mRNAs in *Df(3L)DocA* and *Df(3L)DocB* homozygotes. *Df(3L)DocA* and *Df(3L)DocB* complement female sterility associated with smg^1, whereas *Df(3L)Scf-R6* and *Df(3L)Scf-R11* do not. Therefore upstream *smg* sequences (hatched), including alternative *smg* start sites, are dispensable. The sequences at the breakpoints of *Df(3L)DocA*, *Df(3L)DocB* and *Df(3L)EP584MR2* will be made accessible in FlyBase. (B-D) Mid stage 12 embryos stained with anti-Kr antibody. (B) Embryo homozygous for *Df(3L)DocA* (*DocA* mutant; composite of two focal planes), which lacks Kr in the amnioserosa (arrowheads). Kr in the nervous system serves as an internal staining control (white asterisks). (C) *Doc1+2+3* RNAi embryo, which is a wild-type embryo injected with a mix of *Doc1*, *Doc2* and *Doc3* dsRNA (3′-fragments downstream of T-box) and shows a phenotype as with *DocA* mutants. (D) Control wild-type embryo injected with buffer only. (E) Stage 14 *DocA* mutant embryo showing absence of Kr staining in the amnioserosa region (arrowhead) and incomplete germ band retraction. Somatic muscle staining of Kr in E-G is denoted by black asterisks. (F) Stage 14 *DocA* mutant embryo with forced expression of *Doc2* in the early amnioserosa (via *c381-GAL4*). Kr expression in the amnioserosa is rescued to a significant degree (arrow), as well as extended temporally. Retraction defects are fully rescued in this and the majority of other embryos. (G) Stage 14 *DocA* mutant embryo with forced expression of *Doc3* as in F. There is some rescue of Kr expression in the amnioserosa (arrow) but little rescue of the germ band retraction defects. (H-J) Cuticle preparations of unhatched first instar larvae visualized by dark-field optics. (H) *Df(3L)DocA* mutants have a u-shaped phenotype owing to the failure of germ band retraction. A similar cuticle phenotype is observed in *Doc1+2+3* RNAi embryos (I), but not in the wild-type control (J). as, amnioserosa; fk, filzkörper.

amnioserosa marker *race* (*Ance* – FlyBase) (Tatei et al., 1995) is initiated normally in the primordium of the amnioserosa of *DocA* mutant embryos, suggesting that the expression of the *race* upstream activator *zerknüllt* (*zen*) is also not disrupted (data not shown). However, after embryonic stage 9, *race* expression is gradually lost in the amnioserosa of *DocA* mutant embryos and its residual mRNA distribution closely follows that of Hnt (Fig. 7A, compare with 7B).

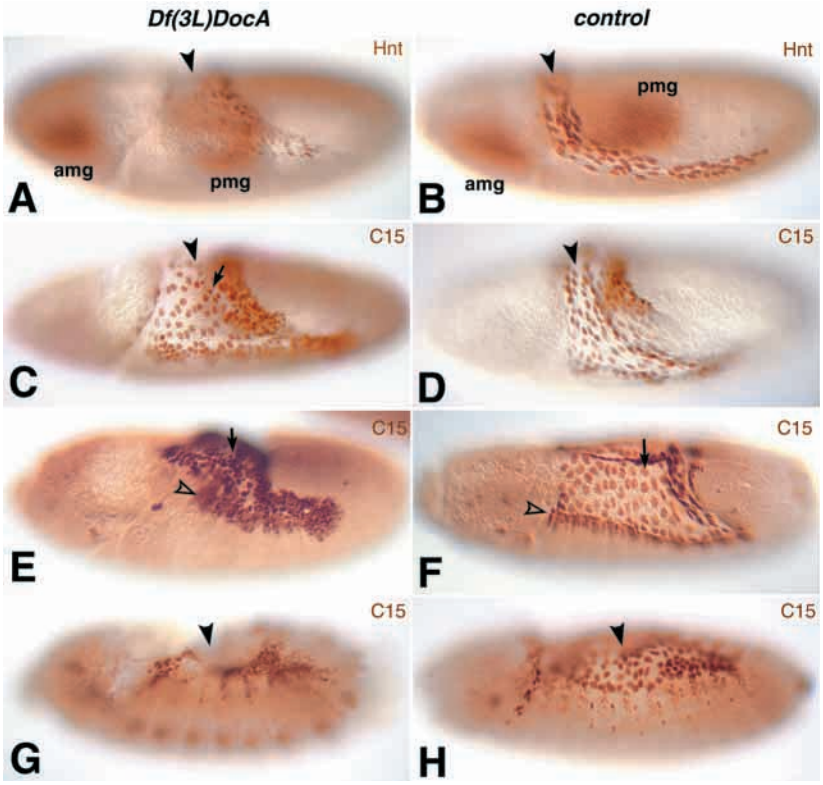

Fig. 6. Loss of Dorsocross causes abnormal development and premature breakdown of the amnioserosa. Homozygous *Df(3L)DocA* mutant embryos (A,C,E,G) and heterozygous control embryos (B,D,F,H) were stained for amnioserosa markers as indicated. (A,B) Expression of *hnt*, as determined with anti-Hnt antibodies, initiates in the absence of Dorsocross (A), but fails to the reach wild-type levels especially in anterior areas of the amnioserosa by stage 9 (arrowheads; compare with B). Note comparable levels of Hnt in midgut primordia (amg, pmg) in A and B. (C-H) Anti-C15 antibody staining of stage 9 (C,D), late stage 12 (E,F) and stage 14 (G,H) embryos. *C15* expression is not reduced in early *DocA* mutants (C) and large flattened nuclei are present in the amnioserosa similar to the wild-type situation (D). However, in *DocA* mutants there are some abnormally small nuclei in the amnioserosa (arrow) and germ band elongation is slightly aberrant. (E) C15 staining of a stage 12 *DocA* mutant embryo reveals a decrease in the size of most amnioserosa nuclei (arrow) and a broadening of the ectodermal C15 expression domain (arrowhead) when compared with F. Around stage 14, no large amnioserosa cells expressing *C15* can be found in *DocA* mutants (G), there is a dorsal hole lacking C15 (arrowhead) and the germ band is not retracted. In the control embryo (H), *C15* expression in the amnioserosa is still strong during this stage and in the dorsal ectoderm it shows a well-defined segmented pattern. *DocA* mutants were initially identified via absence of balancer-derived anti-β-galactosidase staining. Various morphological features (reduction of dorsal head structures, incomplete germ band extension associated with an inwardly kinked posterior germ band, absence of germ band retraction, yolk displacement) were found to be consistently present in mutants, which allows reliable discrimination of mutant and control embryos without anti-β-galactosidase staining after stage 8.

We also examined the expression of a novel amnioserosa marker, which is encoded by the homeobox gene *C15*. In the normal situation, *C15* is expressed in the amnioserosa from stage 7 until stage 17, when the amnioserosa undergoes apoptosis (Fig. 6D,F,H, and data not shown) (Campos-Ortega and Hartenstein, 1997). In addition, from early stage 10 onwards there is a narrow domain of expression at the leading edge of the dorsal germ band, which later becomes segmental (Fig. 6F,H). In *DocA* mutant embryos, the level of *C15* expression in early amnioserosa cells is unaltered, which allows us to use C15 protein as a marker for the development of this tissue in the absence of Doc activity.

Until stage 9, the large majority of amnioserosa nuclei in *DocA* mutant embryos appear large and flattened as in wild-type embryos (Fig. 6C, compare with 6D). Together with data from α-tubulin staining (not shown), this observation indicates that the amnioserosa cells begin to acquire the normal features of a squamous epithelium (data not shown). However, the amnioserosa does not display a properly folded morphology during stages 8-10, and the posterior germ band is forced to bend towards the inside in *DocA* mutant embryos (Fig. 6C, compare with 6D, and data not shown). In addition, some small nuclei become detectable within the amnioserosa during this stage (Fig. 6C, arrow). Altogether, these observations indicate that the amnioserosa initiates its differentiation process in the absence of Doc gene activity but fails to complete it, thus leading to morphological and functional abnormalities of this tissue towards the end of germ band elongation. Much stronger alterations can be observed during subsequent stages, when there are an increasing number of C15-stained amnioserosa nuclei with much smaller diameters than regular amnioserosa nuclei. At late stage 12, almost all amnioserosa cells feature small nuclei that are difficult to distinguish from dorsal epidermal cells (Fig. 6E, Fig. 7C, compare with Fig. 6F, Fig. 7D, respectively). Co-staining for *race* indicates that it is predominantly the cells with the small nuclei that lose *race* expression, while most normally-sized nuclei are still surrounded by *race* signals (Fig. 7C, compare with D). From this stage onwards, non-stained ‘holes’ appear in the amnioserosa and the number of C15-stained amnioserosa nuclei decreases prematurely. Hence, unlike wild-type embryos, stage 14 *DocA* mutant embryos are not covered dorsally by C15-stained amnioserosa cells (Fig. 6G, compare with 6H). In addition to the observed alterations in the amnioserosa, the C15 expression domain at the leading edge of the epidermis appears significantly broadened (Fig. 6E).

We tested whether the increasing number of smaller nuclei in the amnioserosa of *DocA* mutant embryos is connected with abnormal cell divisions. As shown in Fig. 7E, the M-phase marker phospho-Histone H3 can be detected in numerous amnioserosa nuclei of *DocA* mutant embryos after stage 10, which is not seen in wild-type embryos (Fig. 7F). In addition, there is significant incorporation of BrdU in amnioserosa nuclei of *DocA* mutant embryos (particularly

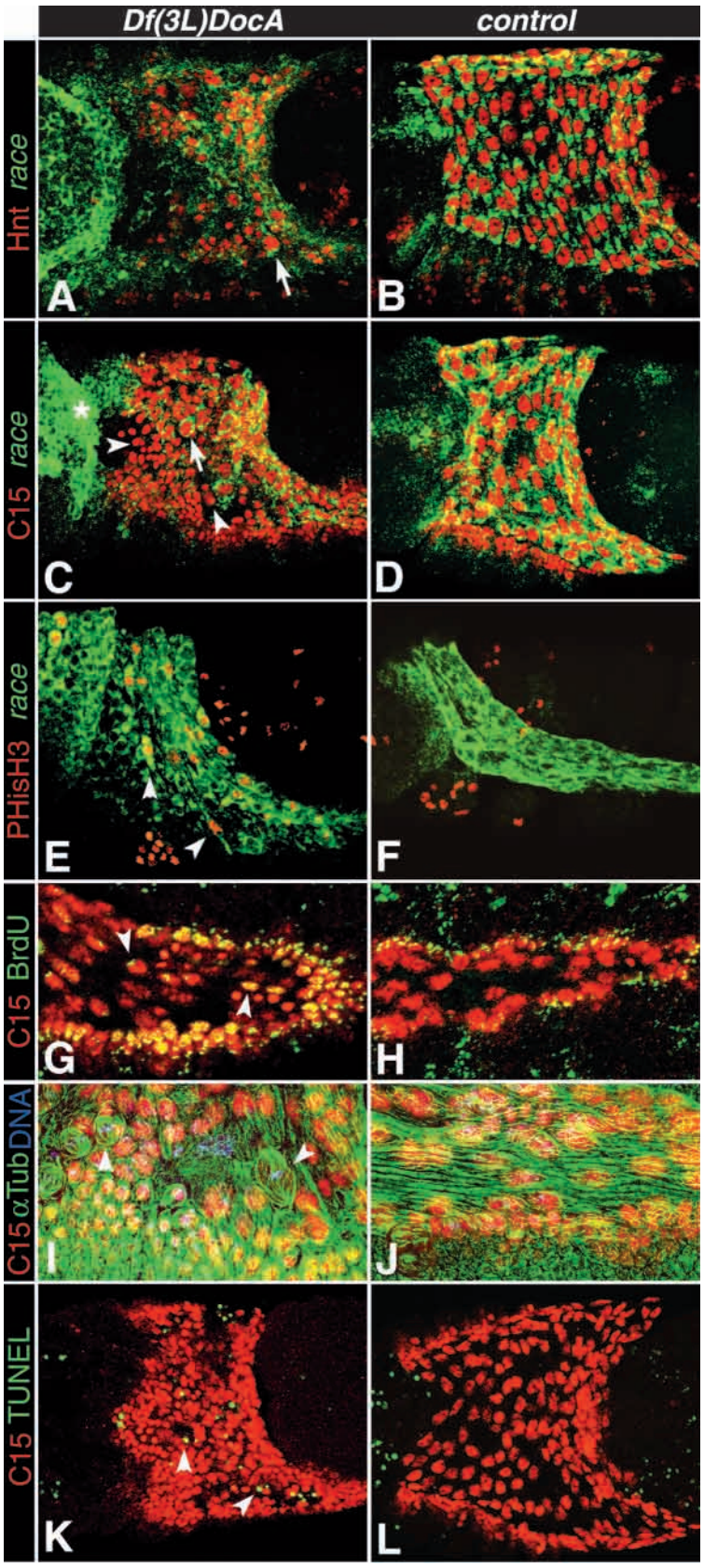

Fig. 7. Abnormal marker expression, cell cycle entry and premature apopotosis of amnioserosa cells in Doc mutant embryos. Shown are confocal fluorescent microscopic images with merged amnioserosa scans. (A-D) *race* in situ hybridization (green) and antibody staining (red) with anti-Hnt (A,B) and anti-C15 (C,D) at stage 12. *race* expression decreases in the amnioserosa of *DocA* mutants. Residual expression of *race* generally correlates with residual Hnt expression (arrow in A) and large C15-stained nuclei (arrow in C; arrowheads, small nuclei). In addition, there are increased levels of *race* mRNA in the posterior/dorsal head (asterisk) of *DocA* embryos. (E,F) Stage 10 embryos stained for *race* mRNA and phospho-Histone H3. Unlike in the wild-type (F), *race*-stained amnioserosa cells show nuclear phospho-Histone H3 staining in *DocA* mutants (E, arrow heads). (G,H) Stage 11 embryos after 30 minutes BrdU pulse labeling, double-stained with anti-BrdU (green) and anti-C15 antibodies (red) to visualize amnioserosa nuclei. Overlapping signals appear yellow. While normal amnioserosa cells are arrested in the G2 phase of cell cycle 14 and do not incorporate BrdU (H), BrdU incorporation is detected in a fraction of amnioserosa cells of *DocA* mutants (arrowheads in G). BrdU incorporation in dorsal ectodermal cells flanking the amnioserosa and other domains is seen in both mutant and wild-type embryos at this stage. (I,J) Stage 11 embryos stained for C15 (red), DNA (Hoechst, blue) and α-tubulin (green) after fixation in the presence of taxol. Mitotic spindles in the amnioserosa of *DocA* mutants (I, arrowheads) indicate dividing amnioserosa cells, which are not seen in wild-type embryos (J). (K,L) Detection of apoptotic cell death in late stage 12 embryos by TUNEL is shown in green and staining with anti-C15 is shown in red. At this stage, there is significant apoptosis within the amnioserosa in *DocA* mutants (K, arrowheads), but none in wild type (L), although apoptosis can be detected in the head and other regions of wild-type embryos. Most apoptotic amnioserosa cells have already lost C15 expression, but are clearly localized within the amniosera layer. Mutant embryos were identified by triple-staining with anti-β-galactosidase (A-D; not shown) or by the absence of anti-Doc2 staining performed in parallel to anti-C15 staining (G,I,K). G,H are at 1.75× greater magnification than A-F,K,L; I,J are at 2.5× greater magnification than A-F,K,L.

in the small nuclei; Fig. 7G), whereas no incorporation is observed in wild-type embryos (Fig. 7H). Mitotic spindles are also present in the amnioserosa of *DocA* mutants (Fig. 7I, compare with J). These observations indicate that the normal G2 arrest of amnioserosa cells has been released and the cells re-enter the cell cycle. We also examined whether the subsequent disappearance of small C15-stained amnioserosa nuclei in *DocA* mutant embryos is a result of premature apoptosis of cells in this tissue. This possibility was confirmed by the results of TUNEL labeling experiments, which produced signals in many amnioserosa nuclei from 12 onwards. Most of the TUNEL-labeled nuclei have reduced or are lacking C15 expression (Fig. 7K, compare with 7L, which shows that wild-type amnioserosa nuclei at late stage 12 are not apoptotic). Altogether, these observations suggest that loss of Doc activity prevents the normal differentiation of the amnioserosa to a fully functional tissue, suspends the cell cycle block of amnioserosa cells, and causes premature apoptotic cell death in this tissue.

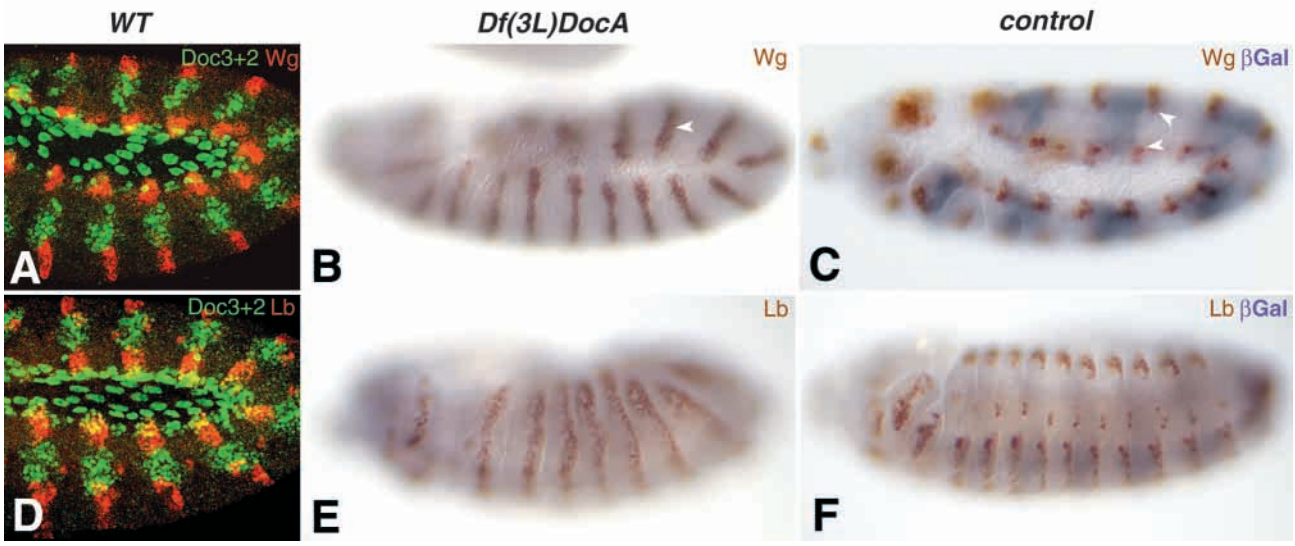

Fig. 8. Dorsocross regulates the patterning of the dorsolateral ectoderm. (A) Fluorescent double-staining with anti-Doc3+2 antibodies (green) and anti-Wg (red). After an initial overlap of expression (see Fig. 4E), at stage 11 there is complementary expression of Doc and *wg* as the *wg* stripes become interrupted in the dorsolateral ectoderm. (B,C) Anti-Wg staining (brown; blue anti-β-galactosidase staining indicates *TM3, eve-lacZ*-balanced control embryos) of stage 11 embryos. Note persistence of continuous stripes in *DocA* mutants (B, arrowhead), which contrasts with interrupted stripes in control embryos (C, arrowheads). (D) Expression of Dorsocross (anti-Doc3+2, green) and *ladybird* (anti-Lbe, red) in the embryonic trunk at stage 11/12. Doc patches are observed between Lb patches similar to the spatial arrangement seen in A. (E,F) Anti-Lbe staining (plus anti-β-galactosidase staining, blue) of stage 14 embryos. (E) Continuous *lb* stripes are visible in the ectoderm of *DocA* mutants. (F) Normal *lb* expression pattern with separated dorsal patches and ventral stripes in the ectoderm in control embryos. Small groups of cells expressing *lb* in the lateral region correspond to muscle precursors.

Doc patterns the lateral ectoderm via repressing *wg* and *ladybird*

The segmental stripes of *wg* expression in the embryonic trunk segments initially span the entire dorsoventral extent of the ectoderm, but at stage 11 they become interrupted in dorsolateral areas (Baker, 1988). A comparison of Wg and Doc expression at this stage shows that the positions of the metameric ectodermal domains of Doc expression correspond to the areas in which the Wg stripes become interrupted (Fig. 8A). Temporally, there is a brief overlap of ectodermal Wg and Doc expression during stage 10 until Wg expression is downregulated within the Doc domains (see Fig. 4E). In contrast to the wild-type situation (Fig. 8A,C), the Wg stripes remain continuous in *DocA* mutant embryos (Fig. 8B). Similar observations were made with the homeobox gene product Ladybird (Lb=Lbe + Lbl) (Jagla et al., 1997) as a marker. In wild-type embryos after stage 11, Lb is also expressed in striped domains that are interrupted at the positions of the ectodermal Doc domains (Fig. 8D), whereas in *DocA* mutant embryos there is ectopic expression in a pattern of continuous stripes (Fig. 8E, compare with F). These data show that Doc activity is required for patterning events in the dorsolateral ectoderm, which include the repression of *wg* and *lb* expression in these areas.

Ectopic expression experiments with Doc genes provide additional evidence for a repressive activity of Doc on *wg* expression. Upon ectopic expression of *Doc2* in all cells of the ectoderm of wild type embryos, the ventral portions of the Wg stripes are lost (Fig. 9B, compare with 9A). However, the dorsal regions of the Wg stripes appear to be under different regulation, because ectopic Doc results in a uniform domain of dorsal Wg along the anteroposterior axis, albeit at lower levels than in wild-type embryos.

Ectopic expression experiments with Doc genes in imaginal discs further confirm their ability to repress *wg*. In third instar larval wing discs, Doc genes are expressed in four distinct areas that do not overlap with the *wg* expression domains. Specifically, two large Doc expression domains are located in the centers of the dorsal and ventral regions of the prospective wing blades and two smaller domains in prospective dorsal hinge and posterior notal regions, respectively (Fig. 9C). In leg discs, low levels of Doc expression can be detected in regions of the prospective body wall and proximal leg segments, which also do not express *wg* (Fig. 9E). Importantly, ectopic expression of *Doc2* within the Dpp domains of imaginal discs causes *wg* expression to disappear in the corresponding areas (Fig. 9D,F). In agreement with the known role of *wg* in limb development (Lecuit and Cohen, 1997), its repression by ectopic Doc results in the loss of distal structures of wings, legs and antenna of adult animals (Fig. 9G-I). Analogous ectopic expression experiments with *Doc1* and *Doc3* in embryos and discs produced qualitatively similar, although weaker, effects to *Doc2*.

DISCUSSION

The closely related T-box sequences, genomic clustering and virtually identical expression patterns of the three Dorsocross genes suggest that they are derived from relatively recent duplications of a common progenitor gene. Accordingly, our observation that loss of *Doc1* or *Doc3* does not cause any of the embryonic phenotypes seen upon loss of all three genes indicates that there is a large degree of functional redundancy among these three genes. Phylogenetic analysis with the

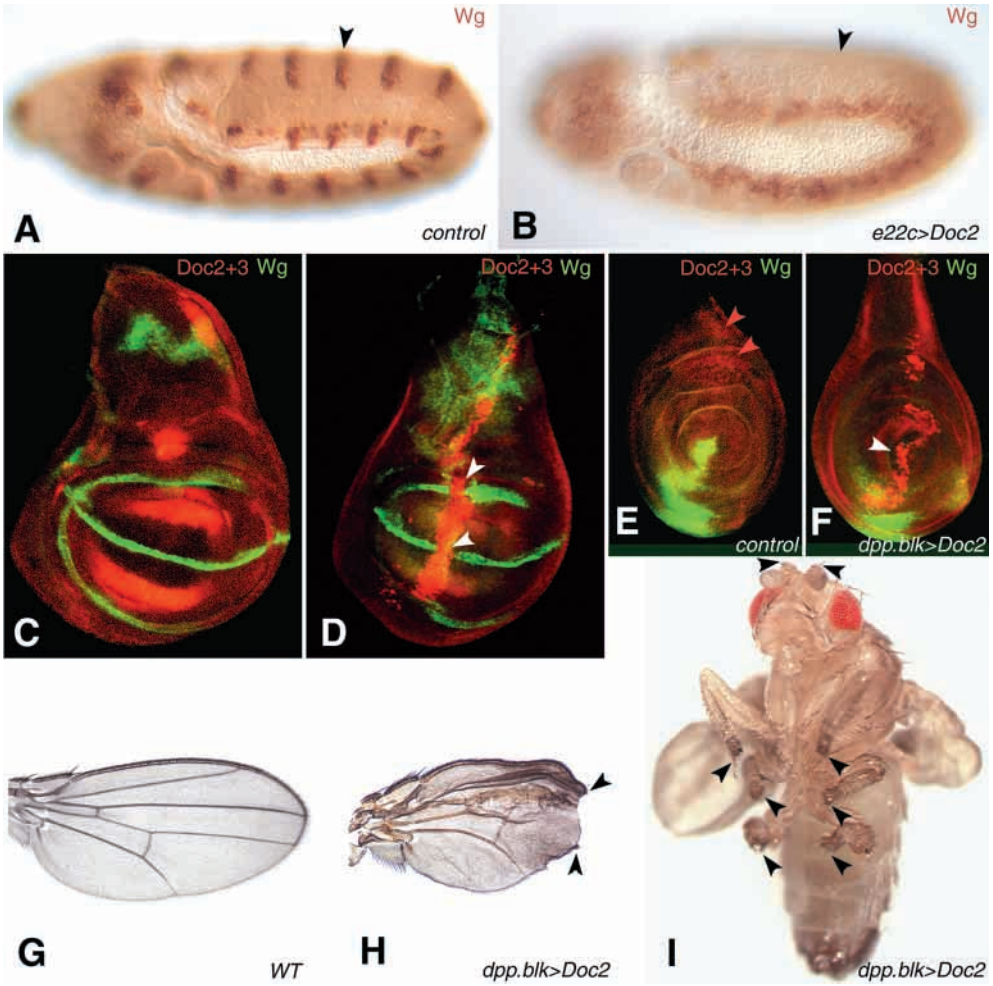

Fig. 9. Ectopic expression of Dorsocross represses *wingless*. (A) *wg* expression in stage 11 control embryo (*UAS-Doc2*/*CyO*). (B) Embryo of similar stage expressing *Doc2* ectopically in the whole ectoderm (*e22c-GAL4*/*UAS-Doc2*). Ventral *wg* expression is missing (see arrowhead) and dorsal *wg* expression is almost continuous, although with reduced levels. (C,D) Dorsocross (red) and *wg* (green) expression in imaginal wing discs from 3rd instar larvae detected by flourescent double-staining using anti-Doc2+3 and anti-Wg antibodies. Dorsal is upwards and anterior towards the left. (C) Wild-type wing disc. (D) Wing discs ectopically expressing *Doc2* in the *dpp* expression domain (*UAS-Doc2*/+;*dpp.blk1-GAL4*/+). Note the interruption of *wg* expression at the intersection of ectopic Doc2 and Wg stripes (arrowheads). (E,F) Leg disc of 3rd instar stained as in C and D. (E) Wild-type leg disc with *wg* expression in anterior/ventral territories. Endogenous Doc protein in dorsal proximal areas of the disc is detected at low levels (red arrowheads). (F) Leg disc from *UAS-Doc2*/+;*dpp.blk1-GAL4*/+ larvae. *wg* expression is repressed by ectopic Doc2 in the central area that normally produces distal parts of the leg (arrowheads). (G) Wild-type wing. (H) Wing derived from a disc with a genotype as in D, which lacks distal structures (arrowheads). Wing veins appear broadened as well. (I) Adult male fly showing a phenotype of intermediate strength caused by ectopic *dpp.blk1*-driven Doc2. Arrowheads indicate aristaless antennae and shortened legs.

extended T-box domain sequences shows that the Doc genes are most closely related to the vertebrate *Tbx6* genes, whose expression in the paraxial mesoderm is reminiscent of the expression of the Doc genes in the dorsal somatic mesoderm. However, the limited reliability of the branches separating the *Tbx6*, *VegT* and *Tbx2* subfamilies in the phylogenetic tree analysis, the absence of *Drosophila* orthologs of *VegT* and *Tbx4/5* genes, as well as shared features of expression in the somatic and/or precardiac and cardiac mesoderm seem to support the alternative possibility that the Doc, *Tbx6*, *VegT* and *Tbx4/5* genes arose from a common ancestral gene by gene amplifactions after the divergence of the insect and vertebrate lineages.

A prominent feature of the Doc genes is their expression in areas that receive inputs from Dpp, including the dorsalmost cells in blastoderm embryos, the dorsolateral ectoderm and mesoderm in the elongated germband, and distinct domains spanning the compartment border of the wing disc. Indeed, our genetic data, together with the co-localization of Doc transcripts with active Mad in dorsal embryonic tissues, favor the possibility that the Doc genes are direct targets of the Dpp signaling cascade. However, the Dpp signals are required to act in combination with additional regulators during each of these inductive events.

Regulation and function of the Doc genes during amnioserosa development

Our observations suggest that robust and stable induction of Doc expression in a dorsal stripe requires the activity of the homeodomain protein Zen as a co-activator of Dpp signals. The *zen* gene features an early, broad expression domain along the dorsal embryonic circumference, which is initially Dpp independent but subsequently requires Dpp for it to be maintained (Rushlow et al., 1987; Ray et al., 1991). Thereafter, its expression refines into a narrow dorsal domain in a process that requires peak levels of Dpp (Rushlow and Levine, 1990; Ray et al., 1991; Rushlow et al., 2001). The activation of Doc expression occurs at the same time as the refinement of *zen* expression and within the same narrow domain, which also coincides with high phospho-Mad levels (Rushlow et al., 2001). Although the maintenance and refinement of *zen* by Dpp is *zen* independent (Ray et al., 1991), we propose that Zen synergizes with peak signals of Dpp to trigger Doc gene expression in a dorsal stripe. The requirement for this proposed

interaction between *zen* and *dpp* would explain the failure of *zen* to activate Doc genes in an early, broad domain as well as the observed low levels of residual Doc expression in *zen* mutant embryos, which may be due to inputs from Dpp alone. Formally, this proposed mechanism would be analogous to previously described inductive events in the early dorsal mesoderm, where the synergistic activities of the homeodomain protein Tinman and activated Smads induce the expression of downstream targets such as *even-skipped* (Halfon et al., 2000; Knirr and Frasch, 2001). The identification of functional binding sites for Zen and Smads in Doc enhancer element(s) will be necessary for demonstrating that an analogous mechanism is active during induction of Doc gene expression in a dorsal stripe. In the absence of such data, we can not completely rule out that dorsal Doc expression is controlled indirectly by *Dpp*, possibly via the combinatorial activities of *zen* and another high-level target gene of Dpp. As mutations in several other genes that are expressed in the early amnioserosa, including *pannier* (*pnr*), *hnt, srp, tup* and *ush*, do not affect Doc expression until at least stage 12 (I.R. and M.F., unpublished), these genes can be excluded as candidates for early upstream regulators of Doc.

Unlike *zen*, which is expressed only transiently, Doc expression is maintained throughout amnioserosa development. Hence, the Doc genes provide a functional link between the early patterning and specification events in dorsal areas of the blastoderm embryo and the subsequent events of amnioserosa differentiation. The activity of *zen* is required for all aspects of amnioserosa development that have been examined to date, including normal activation of *C15* (M.F., unpublished). By contrast, our data demonstrate that the Doc genes execute only a subset of the functions of *zen*, which includes the activation of *Kr* and *hnt*, but not *C15* and early *race*, in amnioserosa cells. This interpretation is consistent with our failure to obtain a significant increase of amnioserosa cells upon ectopic expression of any of the Doc genes in the ectoderm or throughout the early embryo (using *e22c* and *nanos-GAL4* drivers, respectively; I.R. and M.F., unpublished). The residual expression of *hnt* in some amnioserosa cells of Doc mutant embryos could be due to direct inputs from *zen* itself or from a yet undefined *zen* downstream gene acting in parallel with Doc. Nonetheless, the strong reduction of *hnt* expression in Doc mutant embryos could largely account for their amnioserosa-related phenotypes, including the absence of *Kr* expression, the decline of *race* expression, premature apoptosis and failure of germ band retraction. All of these phenotypes have also been observed in *hnt* mutant embryos (Wieschaus et al., 1984; Frank and Rushlow, 1996; Lamka and Lipshitz, 1999; Yip et al., 1997). However, it is likely that Doc gene activity is required for the activation not only of *hnt* but also of additional genes of the u-shaped group and that Doc genes exert some of their functions in parallel with *hnt*. Some evidence for this notion is derived from the observation that loss of Doc activity has a stronger effect on *Kr* expression than loss of *hnt* activity.

One of the hallmarks of amnioserosa development is that the cells of this tissue never resume mitotic divisions after the blastoderm divisions (Campos-Ortega and Hartenstein, 1997). To a large extent, this cell cycle arrest is due to the absence of expression of *cdc25*/*string* in the prospective amnioserosa, which prevents the cells from entering M-phase and leads to G2 arrest (Edgar and O'Farrell, 1989). In addition, the expression of the Cdk inhibitor p21/Dacapo in the early amnioserosa is thought to contribute to the cell cycle arrest (de Nooij et al., 1996; Lane et al., 1996). Although a detailed description of the regulation of *string* and *dacapo* expression in dorsal embryonic areas is lacking, it has been reported that *zen* is required for repressing dorsal *string* expression, which is expected to prevent further cell divisions (Edgar and O'Farrell, 1990; Edgar et al., 1994). Notably, our observation that amnioserosa cells re-enter the cell cycle in Doc mutant embryos demonstrate that Doc genes are required for the cell cycle block in addition to *zen*. Whereas *zen* mutant embryos feature ectopic cell divisions in dorsal areas already from stage 8 onwards (Arora and Nüsslein-Volhard, 1992), in Doc mutants the amnioserosa cells resume mitosis only during and after stage 10, which is shortly after Zen protein disappears. Thus, we hypothesize that the Doc genes take over the function of *zen* in repressing *string* and prevent cell divisions at later stages of amnioserosa development when Zen is no longer present. Overall, the phenotype of Doc mutant embryos suggests that amnioserosa differentiation, including cell cycle arrest and the development of squamous epithelial features, initiates in the absence of Doc activity but is not maintained beyond stage 11. Thereafter, cell division resumes and there is a reversal of the partially differentiated state. Apoptotic events are not observed prior to stage 11 in Doc mutants. However at later stages, many amnioserosa cells die prematurely and the remaining cells are difficult to distinguish morphologically from dorsal ectodermal cells.

Altogether, our studies have identified the Doc genes as new members of the u-shaped group of genes, which control amnioserosa development, and provide new insights into the regulatory pathways in amnioserosa development downstream of Dpp (summarized in Fig. 10) (see also Rusch and Levine, 1997). In future studies, it will be necessary to define the specific roles of the remaining genes of the u-shaped family, particularly *ush*, *srp*, *tup* and *C15*, in this regulatory framework in more detail.

Regulation and function of the Doc genes during patterning of lateral epidermis and dorsal mesoderm

Unlike in the presumptive amnioserosa, not all cells in the

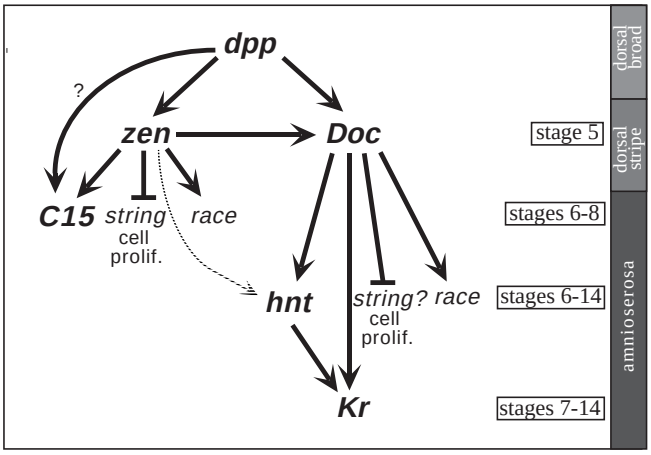

Fig. 10. Summary of currently known regulatory networks during amnioserosa development. Dorsocross genes act downstream of *Dpp* and *zen*, and upstream of *hnt* and *Kr*. Other pathways, which include *C15*, act in parallel with Dorsocross (see Discussion).

dorsolateral ectoderm and dorsal mesoderm that receive high levels of Dpp induce Doc expression. Rather, Wg signals are required in combination with Dpp in these tissues, such that the Doc genes are induced at the intersections of transverse Wg stripes and the dorsally restricted domain containing high phospho-Mad levels. The Doc stripes extend beyond the peak levels of Wg on both sides of the Wg stripes, which indicates that the Doc genes are able to respond to relatively low levels of diffusible Wg. In addition, the absence of Doc expression in the dorsalmost cells of the ectoderm that receive Wg and Dpp signals indicates the presence of a negative regulator that prevents Doc induction in the ectoderm adjacent to the amnioserosa until stage 12. Together, these inputs restrict Doc expression to metameric quadrants that encompass the areas of the dorsolateral ectoderm between the tracheal placodes as well as the underlying mesodermal cells.

Previous studies have shown that some of the effects of *wg* are mediated by its target gene *sloppy paired* (*slp*), including the feedback activation of *wg* in the ectoderm and the repression of *bagpipe* (*bap*) in the mesoderm (Cadigan et al., 1994; Lee and Frasch, 2000). However, the residual (although strongly reduced) expression of the Doc genes in the germ band of *slp* mutant embryos argues against a role of *slp* in mediating the function of *wg* to induce the Doc genes. Hence, the Doc genes may be direct targets of the Wg signaling cascade in the ectoderm and mesoderm.

Our observations show that one of the important functions of the Doc genes in the dorsolateral ectoderm is the repression of *wg* expression. Although the expression of Doc initially depends on *wg*, the Doc genes subsequently exert a negative feedback on *wg* expression, which leads to the previously unexplained interruption of the *wg* stripes during stage 11. Because the ventral extent of the ectodermal Doc domains correlates with the ventral borders of high levels of P-Mad, we conclude that the dorsal limit of the ventral *wg* stripes at stage 11 is determined indirectly by Dpp via Doc.

The maintenance of *wg* after stage 10 has been shown to depend on two different positive feedback loops, one being active in the dorsal and the other in the ventral ectoderm. The dorsal feedback loop is mediated by the *ladybird* homeobox genes (*lb=lbe* and *lbl*), whereas the ventral loop is mediated by the Pax gene *gooseberry* (*gsb*) (Li and Noll, 1993; Jagla et al., 1997). The Doc genes must interrupt one or both of these feedback loops, although it is not clear whether the primary block is at the level of the *wg* gene or at the level of the transcription factor-encoding genes *lb* and/or *gsb*. Another target for repression by the Doc genes in this pathway could be *slp*, which is required both dorsally and ventrally in *wg* feedback regulation (Cadigan et al., 1994; Lee and Frasch, 2000). We think that *lb* is unlikely to be the primary target of Doc repression as the failure of *wg* repression temporally precedes the expansion of the *lb* stripes in Doc mutant embryos. Furthermore, our observation that the Doc genes can also repress *wg* in other tissue contexts such as the imaginal discs, where *gsb*, *lb* and *slp* are not components of a *wg* feedback loop, seems to favor the mechanism of a direct repression of the *wg* gene by Doc.

Taken together, our observations show that dynamic interactions among positive and negative feedback loops, which share *wg* as a common component, are involved in the dorsoventral and anteroposterior patterning of the embryonic ectoderm. The activity of the Doc genes in negatively regulating *wg* and *lb*, as well as their potential positive effects on yet unknown targets in the dorsolateral ectoderm, are expected to be important for the proper dorsoventral organization of the cuticle and sensory organs. In the mesoderm, the metameric expression domains of the Doc genes during stages 9-11 include the dorsal somatic and cardiac mesoderm. Notably, preliminary analysis has revealed defects in dorsal somatic muscle and dorsal vessel development in Doc mutant embryos, which we are currently examining in more detail. Finally, we note that the expression pattern of the Doc genes in the embryonic epidermis is very reminiscent of the pattern of expression and activity of another T-box gene, *optomotor-blind* (*omb*), in the pupal epidermis (Kopp and Duncan, 1997). Doc and *omb* expression overlap in the wing discs although, unlike *omb*, Doc expression is interrupted near the Wg domains (Grimm and Pflugfelder, 1996). Furthermore, it has been reported that dominant mutations in the gene *Scruffy* (*Scf*) and their revertants genetically interact with *omb* during abdominal cuticle and wing patterning (Kopp and Duncan, 1997). Because we have mapped the breakpoints of two *Scf* revertants, *Df(3L)Scf-R6* and *Scf-R11*, directly upstream and downstream, respectively, of the *Doc3* gene, it is tempting to speculate that the *Scf* phenotype is caused by rearranged *Doc3*. Future studies will clarify the relationship between *Scf* and Doc genes and establish whether the T-box genes Doc and *omb* functionally interact during patterning of the adult cuticle and wings.

We thank the Bloomington stock center for fly stocks; K. Jagla, D. Kosman, J. Reinitz, C. Rushlow and the Developmental Studies Hybridoma Bank (University of Iowa/NICHD) for antibodies and probes; and D. Kosman for the double-in situ hybridization protocol. This research was supported by a grant to M.F. from the National Institutes of Health (HD30832). The Mount Sinai Confocal Microscopy Shared Resource Facility was supported, in part, with funding from NIH-NCI shared resources grant (1 R24 CA095823-01).

REFERENCES

Adams, M. D., Celniker, S. E., Holt, R. A., Evans, C. A., Gocayne, J. D., Amanatides, P. G., Scherer, S. E., Li, P. W., Hoskins, R. A., Galle, R. F. et al. (2000). The genome sequence of *Drosophila melanogaster*. *Science* **287**, 2185-2195.

Anderson, M., Perkins, G., Chittick, P., Shrigley, R. and Johnson, W. (1995). *drifter*, a *Drosophila* POU-domain transcription factor, is required for correct differentiation and migration of tracheal cells and midline glia. *Genes Dev.* **9**, 123-137.

Arora, K., Levine, M. and O'Connor, M. (1994). The *screw* gene encodes a ubiquitously expressed member of the TGF-β family required for specification of dorsal cell fates in the *Drosophila* embryo. *Genes Dev.* **8**, 2588-2601.

Arora, K. and Nüsslein-Volhard, C. (1992). Altered mitotic domains reveal fate map changes in *Drosophila* embryos mutant for zygotic dorsoventral patterning genes. *Development* **114**, 1003-1024.

Ashe, H. and Levine, M. (1999). Local inhibition and long-range enhancement of Dpp signal transduction by Sog. *Nature* **398**, 427-431.

Ashe, H., Mannervik, M. and Levine, M. (2000). Dpp signaling thresholds in the dorsal ectoderm of the *Drosophila* embryo. *Development* **127**, 3305-3312.

Azpiazu, N. and Frasch, M. (1993). *tinman* and *bagpipe*: two homeo box genes that determine cell fates in the dorsal mesoderm of *Drosophila*. *Genes Dev.* **7**, 1325-1340.

Azpiazu, N., Lawrence, P., Vincent, J.-P. and Frasch, M. (1996). Segmentation and specification of the *Drosophila* mesoderm. *Genes Dev.* **10**, 3183-3194.

Baker, N. E. (1988). Transcription of the segment-polarity gene wingless in

the imaginal discs of *Drosophila*, and the phenotype of a pupal-lethal wingless mutation. *Development* **102**, 489-497.

Bodmer, R. (1993). The gene *tinman* is required for specification of the heart and visceral muscles in *Drosophila*. *Development* **118**, 719-729.

Brand, A. H. and Perrimon, N. (1993). Targeted gene expression as a means of altering cell fates and generating dominant phenotypes. *Development* **118**, 401-415.

Brown, N. H. and Kafatos, F. C. (1988). Functional cDNA libraries from *Drosophila* embryos. *J. Mol. Biol.* **203**, 425-437.

Cadigan, K., Grossniklaus, U. and Gehring, W. (1994). Localized expression of *sloppy paired* protein maintains the polarity of *Drosophila* parasegments. *Development* **8**, 899-913.

Campos-Ortega, J. A. and Hartenstein, V. (1997). *The Embryonic Development of* Drosophila melanogaster. Berlin: Springer Verlag.

Carmena, A., Gisselbrecht, S., Harrison, J., Jimenez, F. and Michelson, A. (1998). Combinatorial signaling codes for the progressive determination of cell fates in the *Drosophila* embryonic mesoderm. *Genes Dev.* **15**, 3910-3922.

Dahanukar, A., Walker, J. A. and Wharton, R. P. (1999). Smaug, a novel RNA-binding protein that operates a translational switch in *Drosophila*. *Mol. Cell* **4**, 209-218.

de Nooij, J., Letendre, M. and Hariharan, I. (1996). A cyclin-dependent kinase inhibitor, Dacapo, is necessary for timely exit from the cell cycle during *Drosophila* embryogenesis. *Cell* **87**, 1237-1247.

Decotto, E. and Ferguson, E. (2001). A positive role for Short gastrulation in modulating BMP signaling during dorsoventral patterning in the *Drosophila* embryo. *Development* **128**, 3831-3841.

Doyle, H. J., Harding, K., Hoey, T. and Levine, M. (1986). Transcripts encoded by a homoeo box gene are restricted to dorsal tissues of *Drosophila* embryos. *Nature* **323**, 76-79.

Duan, H., Skeath, J. B. and Nguyen, H. T. (2001). *Drosophila* Lame duck, a novel member of the Gli superfamily, acts as a key regulator of myogenesis by controlling fusion-competent myoblast development. *Development* **128**, 4489-4500.

Edgar, B., Lehman, D. and O'Farrell, P. (1994). Transcriptional regulation of *string* (*cdc25*): a link between developmental programming and the cell cycle. *Development* **120**, 3131-3143.

Edgar, B. and O'Farrell, P. (1989). Genetic control of cell division patterns in the *Drosophila* embryo. *Cell* **57**, 177-187.

Edgar, B. A. and O'Farrell, P. H. (1990). The three postblastoderm cell cycles of *Drosophila* embryogenesis are regulated in G2 by *string*. *Cell* **62**, 469-480.

Ferguson, E. and Anderson, K. (1992a). decapentaplegic acts as a morphogen to organize dorsal-ventral pattern in the *Drosophila* embryo. *Cell* **71**, 451-461.

Ferguson, E. L. and Anderson, K. V. (1992b). Localiced enhancement and repression of the activity of the TGF-ß family member, *decapentaplegic*, is necessary for dorsal-ventral pattern formation in the *Drosophila* embryo. *Development* **114**, 583-597.

Francois, V., Solloway, M., O'Neill, J., Emery, J. and Bier, E. (1994). Dorsal-ventral patterning of the *Drosophila* embryo depends on a putative negative growth factor encoded by the *short gastrulation* gene. *Genes Dev.* **8**, 2602-2616.

Frank, L. and Rushlow, C. (1996). A group of genes required for maintenance of amnioserosa tissue in *Drosophila*. *Development* **122**, 1343-1352.

Frasch, M. (1995). Induction of visceral and cardiac mesoderm by ectodermal Dpp in the early *Drosophila* embryo. *Nature* **374**, 464-467.

Garcia Abreu, J., Coffinier, C., Larrain, J., Oelgeschlager, M. and de Robertis, E. (2002). Chordin-like CR domains and the regulation of evolutionarily conserved extracellular signaling systems. *Gene* **287**, 39-47.

Goldman-Levi, R., Miller, C., Greenberg, G., Gabai, E. and Zak, N. (1996). Cellular pathways acting along the germband and in the amnioserosa may participate in germband retraction of the *Drosophila melanogaster* embryo. *Int. J. Dev. Biol.* **40**, 1043-1051.

Grimm, S. and Pflugfelder, G. (1996). Control of the gene o*ptomotor-blind* in *Drosophila* wing development by *decapentaplegic* and *wingless*. *Science* **271**, 1601-1604.

Halfon, M., Carmena, A., Gisselbrecht, S., Sackerson, C., Jimenez, F., Baylies, M. and Michelson, A. (2000). Ras pathway specificity is determined by the integration of multiple signal-activated and tissue-restricted transcription factors. *Cell* **103**, 63-74.

Huang, A. M., Rehm, E. J. and Rubin, G. M. (2000). Recovery of DNA sequences flanking P-element insertions: inverse PCR and plasmid rescue. In Drosophila *Protocols* (ed. W. Sullivan, M. Ashburner and R. S. Hawley), pp. 429-438. Cold Spring Harbor, New York: Cold Spring Harbor Laboratory Press.

Irish, V. F. and Gelbart, W. M. (1987). The *decapentaplegic* gene is required for dorsal-ventral patterning of the *Drosophila* embryo. *Genes Dev.* **1**, 868-879.

Jagla, K., Jagla, T., Heitzler, P., Dretzen, G., Bellard, F. and Bellard, M. (1997). *ladybird*, a tandem of homeobox genes that maintain late *wingless* expression in terminal and dorsal epidermis of the *Drosophila* embryo. *Development* **124**, 91-100.

Jazwinska, A., Rushlow, C. and Roth, S. (1999). The role of *brinker* in mediating the graded response to Dpp in early *Drosophila* embryos. *Development* **126**, 3323-3334.

Kennerdell, J. R. and Carthew, R. W. (1998). Use of dsRNA-mediated genetic interference to demonstrate that *frizzled* and *frizzled 2* act in the Wingless pathway. *Cell* **95**, 1017-1026.

Kirkpatrick, H., Johnson, K. and Laughon, A. (2001). Repression of *dpp* targets by binding of Brinker to Mad sites. *J. Biol. Chem.* **276**, 18216-18222.

Klapper, R., Stute, C., Schomaker, O., Strasser, T., Janning, W., Renkawitz-Pohl, R. and Holz, A. (2002). The formation of syncytia within the visceral musculature of the *Drosophila* midgut is dependent on *duf, sns* and *mbc*. *Mech. Dev.* **110**, 85-96.

Knirr, S., Azpiazu, N. and Frasch, M. (1999). The role of the NK-homeobox gene *slouch* (*S59*) in somatic muscle patterning. *Development* **126**, 4525-4535.

Knirr, S. and Frasch, M. (2001). Molecular integration of inductive and mesoderm-intrinsic inputs governs *even-skipped* enhancer activity in a subset of pericardial and dorsal muscle progenitors. *Dev. Biol.* **238**, 13-26.

Kopp, A. and Duncan, I. (1997). Control of cell fate and polarity in the adult abdominal segments of *Drosophila* by *optomotor-blind*. *Development* **124**, 3715-3726.

Kosman, D., Small, S. and Reinitz, J. (1998). Rapid preparation of a panel of polyclonal antibodies to *Drosophila* segmentation proteins. *Dev. Genes Evol.* **208**, 290-294.

Lamka, M. and Lipshitz, H. (1999). Role of the amnioserosa in germ band retraction of the *Drosophila melanogaster* embryo. *Dev. Biol.* **214**, 102-112.

Lane, M., Sauer, K., Wallace, K., Jan, Y., Lehner, C. and Vaessin, H. (1996). Dacapo, a cyclin-dependent kinase inhibitor, stops cell proliferation during *Drosophila* development. *Cell* **87**, 1225-1235.

Lecuit, T. and Cohen, S. (1997). Proximal-distal axis formation in the Drosophila leg. *Nature* **388**, 139-145.

Lee, H. and Frasch, M. (2000). Wingless effects mesoderm patterning and ectoderm segmentation events via induction of its downstream target *sloppy paired*. *Development* **127**, 5497-5508.

Li, X. and Noll, M. (1993). Role of the *gooseberry* gene in *Drosophila* embryos: maintenance of *wingless* expression by a *wingless-gooseberry* autoregulatory loop. *EMBO J.* **12**, 4499-4509.

Lo, P. C. and Frasch, M. (2001). A role for the *COUP-TF*-related gene *seven-up* in the diversification of cardioblast identities in the dorsal vessel of *Drosophila*. *Mech. Dev.* **104**, 49-60.

Manseau, L., Baradaran, A., Brower, D., Budhu, A., Elefant, F., Phan, H., Philip, A. V., Yang, M., Glover, D., Kaiser, K., Palter, K. and Selleck, S. (1997). GAL4 enhancer traps expressed in the embryo, larval brain, imaginal discs, and ovary of *Drosophila*. *Dev. Dyn.* **209**, 310-322.

Mason, E., Konrad, K., Webb, C. and Marsh, J. (1994). Dorsal midline fate in *Drosophila* embryos requires twisted gastrulation, a gene encoding a secreted protein related to human connective tissue growth factor. *Genes Dev.* **8**, 1489-1501.

Papaioannou, V. (2001). T-box genes in development: From hydra to humans. *Int. Rev. Cytol.* **207**, 1-69.

Preston, C., Sved, J. and Engels, W. (1996). Flanking duplications and deletions associated with *P*-induced male recombination in *Drosophila*. *Genetics* **144**, 1623-1638.

Ray, R., Arora, K., Nüsslein-Volhard, C. and Gelbart, W. M. (1991). The control of cell fate along the dorsal-ventral axis of the *Drosophila* embryo. *Development* **113**, 35-54.

Riechmann, V., Irion, U., Wilson, R., Grosskortenhaus, A. and Leptin, M. (1997). Control of cell fates and segmentation in the *Drosophila* mesoderm. *Development* **124**, 2915-2922.

Rubin, G. M. and Spradling, A. C. (1982). Genetic transformation of *Drosophila* with transposable element vectors. *Science* **218**, 348-353.

Rusch, J. and Levine, M. (1997). Regulation of a *dpp* target gene in the *Drosophila* embryo. *Development* **127**, 303-311.

Rushlow, C., Frasch, M., Doyle, H. and Levine, M. (1987). Maternal

regulation of zerknüllt: a homoeobox gene controlling differentiation of dorsal tissues in *Drosophila*. *Nature* **330**, 583-586.

Rushlow, C. and Levine, M. (1990). Role of the *zerknüllt* gene in dorsal-ventral pattern formation in *Drosophila*. *Adv. Genet.* **27**, 277-307.

Rushlow, C., Colosimo, P., Lin, M.-C., Xu, M. and Kirov, N. (2001). Transcriptional regulation of the *Drosophila* gene *zen* by competing Smad and Brinker inputs. *Genes Dev.* **15**, 340-351.

San Martin, B., Ruiz-Gomez, M., Landgraf, M. and Bate, M. (2001). A distinct set of founders and fusion-competent myoblasts make visceral muscles in the *Drosophila* embryo. *Development* **128**, 3331-3338.

Sherman, A. W. (2000). BrdU labeling of chromsomes. In Drosophila *Protocols* (ed. W. Sullivan, M. Ashburner and R. S. Hawley), pp. 57-65. Cold Spring Harbor, NY: Cold Spring Harbor Laboratory Press.

Sivasankaran, R., Vigano, M., Muller, B., Affolter, M. and Basler, K. (2000). Direct transcriptional control of the Dpp target *omb* by the DNA binding protein Brinker. *EMBO J.* **19**, 6162-6172.

St Johnston, R. D. and Gelbart, W. M. (1987). *Decapentaplegic* transcripts are localized along the dorsal-ventral axis of the *Drosophila* embryo. *EMBO J.* **6**, 2785-2791.

Staehling-Hampton, K., Hoffmann, F. M., Baylies, M. K., Rushton, E. and Bate, M. (1994). *dpp* induces mesodermal gene expression in *Drosophila*. *Nature* **372**, 783-786.

Su, M., Fujioka, M., Goto, T. and Bodmer, R. (1999). The *Drosophila* homeobox genes *zfh-1* and *even-skipped* are required for cardiac-specific differentiation of a *numb*-dependent lineage decision. *Development* **126**, 3241-3251.

Tatei, K., Cai, H., Ip, Y. and Levine, M. (1995). Race: a Drosophila homolog of the angiotensin converting enzyme. *Mech. Dev.* **51**, 157-168.

Tracey, W. D., Jr, Ning, X., Klingler, M., Kramer, M. and Gergen, J. P. (2000). Quantitative analysis of gene function in the *Drosophila* embryo. *Genetics* **154**, 273-284.

Wieschaus, E., Nüsslein-Volhard, C. and Jürgens, G. (1984). Mutations affecting the pattern of the larval cuticle in *Drosophila melanogaster* III. Zygotic loci on the X-chromosome and fourth chromosome. *Roux's Arch. Dev. Biol.* **193**, 296-307.

Wu, X., Golden, K. and Bodmer, R. (1995). Heart development in *Drosophila* requires the segment polarity gene *wingless*. *Dev. Biol.* **169**, 619-628.

Xu, X., Yin, Z., Hudson, J., Ferguson, E. and Frasch, M. (1998). Smad proteins act in combination with synergistic and antagonistic regulators to target Dpp responses to the *Drosophila* mesoderm. *Genes Dev.* **12**, 2354-2370.

Yip, M., Lamka, M. and Lipshitz, H. (1997). Control of germ-band retraction in *Drosophila* by the zinc-finger protein HINDSIGHT. *Development* **124**, 2129-2141.

Zaffran, S., Küchler, A., Lee, H. H. and Frasch, M. (2001). *biniou* (*FoxF*), a central component in a regulatory network controlling visceral mesoderm development and midgut morphogenesis in *Drosophila*. *Genes Dev.* **15**, 2900-2915.

Zhang, H., Levine, M. and Ashe, H. (2001). Brinker is a sequence-specific transcriptional repressor in the *Drosophila* embryo. *Genes Dev.* **15**, 261-266.